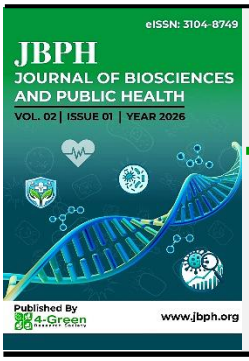

J. Biosci. Public Health 2026; 2(1):30-54

JBPH

Open access

Journal of Biosciences and Public Health

eISSN: 3104-8749

DOI: https://doi.org/10.5455/JBPH.2025.20

Published by: www.4greenresearch.org

Original Research

Decoding Genome, Phylogenetic Insights, Plant-Beneficial Genetic Repertoire, and *In Silico* Pesticide Biodegradation Pathways of Endophytic strain *Serratia* sp. HSTU-ABk35

Md. Shohorab Hossain[1,2], Shahinur Alam[1], Lizzy Mwamburi[3], Aminur Rahman[4], Bissas Binduraz[1], Sukumar Roy[1], Mst. Tahsin Sultana[1], Sibdas Ghosh[5], Md. Azizul Haque[1]*

[1]Department of Biochemistry and Molecular Biology, Hajee Mohammad Danesh Science and Technology University, Dinajpur 5200, Bangladesh
[2]Department of Biochemistry and Molecular Biology, Trust University, Barishal, Bangladesh
[3]Department of Plant Pathology, University of Eldoret, Keniya
[4]Department of Biomedical Sciences, College of Clinical Pharmacy, King Faisal University, Saudi Arabia
[5]Albany College of Pharmacy and Health Sciences, 106 New Scotland Avenue, Albany, NY 12208, United States of America

Article information
Received: November 26, 2025
Revised: December 15, 2025
Accepted: December 15, 2025
Published: December 16, 2025

***Corresponding author**
Department of Biochemistry and Molecular Biology, Hajee Mohammad Danesh Science and Technology University, Dinajpur5200, Bangladesh
E-mail: helalbmb2016@hstu.ac.bd
ORCID ID: https://orcid.org/0000- 0002-9788-0766

Keywords: Serratia sp., Endophyte, Genome sequencing, Pesticide degradation, Plant growth promotion

Cite this article: Hossain MS, Alam S, Wmburry L, Rahman A, Binduraz B, Roy S, Sultana MT, Ghosh S, Haque MA. Decoding genome, phylogenetic insights, plant-beneficial genetic repertoire, and in-silico pesticide biodegradation pathways of endophytic strain *Serratia* sp. HSTU-ABk35. **J Biosci Public Health.** 2026;2(1):30-54. doi:10.5455/JBPH.2025.20

ABSTRACT

Endophytic bacteria are key mediators of plant growth promotion and pesticide detoxification, yet the genomic mechanisms enabling these dual functions remain underexplored. This study is aimed at exploring new endophytic strains from rice plants from pesticides contaminated soil with their genomic insights. Here, we report the whole-genome sequencing and in-silico functional characterization of *Serratia* sp. HSTU-ABk35, an endophyte isolated from rice plants (*Oryza sativa*). Genome analysis revealed a 5.18 Mb chromosome with a GC content characteristic of *Serratia*, harboring coding sequences associated with phytohormone biosynthesis, ACC deaminase activity, siderophore production, phosphate solubilization, oxidative stress tolerance, and systemic resistance induction. Phylogenomic analyses based on ANI, dDDH, and housekeeping genes (*rec*A, *gyr*B, *rpo*B, and 16S rRNA) indicate that *Serratia* sp. HSTU-ABk35 closely related to *Serratia marcescens* but exhibits notable evolutionary divergence, suggesting novel genomic features potentially associated with its endophytic lifestyle and agrochemical adaptability. Functional annotation identified an array of xenobiotic-degrading genes, including esterases, amidohydrolases, α/β-hydrolases, and phosphonate-metabolizing operons, implicating the strain in the degradation of organophosphate, pyrethroid, and carbamate pesticides. Virtual screening and molecular docking of key pesticide-degrading proteins confirmed strong binding affinity and plausible enzyme–pesticide interactions, supporting the predicted biotransformation potential. Collectively, the genomic novelty and functional versatility of *Serratia* sp. HSTU-ABk35 highlight its promise as a multifunctional endophyte with potential applications in sustainable agriculture, including crop growth promotion, stress tolerance enhancement, and bioremediation of pesticide-contaminated soils.

1. INTRODUCTION

Endophytic bacteria colonize internal plant tissues without causing apparent harm, providing multifaceted benefits such as plant growth promotion, biocontrol against phytopathogens, and bioremediation of environmental pollutants [1-3]. These microbes enhance nutrient acquisition through phytohormone production (e.g., indole-3-acetic acid), phosphate solubilization, nitrogen fixation, and induction of systemic resistance, thereby boosting crop resilience to abiotic and biotic stresses [4-6]. In sustainable agriculture, endophytes reduce reliance on chemical inputs, helping address global challenges like soil salinity, drought, and pesticide accumulation [7, 8]. Their ability to adapt to diverse and often harsh environmental conditions further positions them as potent alternatives to conventional synthetic fungicides and chemical fertilizers [9].

The genus *Serratia* exemplifies versatile plant-associated bacteria that inhabit diverse niches, including soil, water, the rhizosphere, and the endosphere [10, 11]. Although some strains act as opportunistic pathogens, many possess plant growth-promoting traits such as IAA biosynthesis, siderophore production, phosphate solubilization, and antagonism through secondary metabolites like prodigiosin, chitinases, proteases, and non-ribosomal peptides [11, 12]. These *Serratia* endophytes promote root and shoot growth, alleviate heavy metal toxicity, and suppress pathogens such as *Fusarium* and *Rhizoctonia* via competition, antibiosis, and induced systemic resistance [11, 12]. Moreover, genomic studies have revealed conserved gene clusters for iron scavenging, quorum sensing, and biofilm formation, all of which facilitate plant colonization [13-15].

Pesticide overuse contaminates agroecosystems, posing risks to soil health, biodiversity, and human welfare. Microbial degradation offers eco-friendly remediation, with endophytes accessing pollutants via plant uptake [16, 17]. *Serratia* strains degrade chlorinated pesticides (e.g., chlorpyrifos), PAHs (e.g., benzo(a)pyrene), and insecticides via enzymatic pathways involving hydrolases, monooxygenases, and dehalogenases [16-18]. Phylogenomics elucidates *Serratia* evolution, with 16S rRNA, *gyrB*, and core-genome trees placing plant-beneficial strains in distinct clades alongside biocontrol species like *S. plymuthica* and *S. marcescens* [10, 19, 20]. Although rice endophytes have been extensively investigated for their diversity and functional roles [1-4], endophytic bacteria with confirmed pesticide-degrading capabilities remain poorly characterized and relatively rare. This critical knowledge gap limits the development of effective, eco-friendly bioremediation strategies for pesticide-contaminated agricultural systems. The discovery and characterization of novel pesticide-degrading endophytes are therefore of significant importance for sustainable agriculture, as such microbes can provide dual benefits by facilitating in planta pesticide detoxification while simultaneously enhancing crop resilience under chemically stressed agroecosystems.

In this study, we present an in-depth genomic analysis of the endophytic strain *Serratia* sp. HSTU-ABk35, isolated from healthy rice plants (*Oryza sativa*) tissues. We characterize its taxonomic position, evolutionary relationships, and plant-beneficial genetic repertoire using state-of-the-art computational tools. Furthermore, we decode the in-silico mechanisms associated with the degradation of major classes of pesticides by identifying putative catabolic genes and metabolic pathways. The findings offer novel insights into the dual functional potential of *Serratia* sp. HSTU-ABk35 and highlight

its prospects for development as a next-generation bioinoculant with both plant growth-promoting and bioremediation capabilities.

2. MATERIALS AND METHODS

2.1. Isolation and biochemical characterization of endophytic bacteria from rice plants

Endophytic bacterial strains, specifically *Serratia* sp. HSTU-ABK35, was isolated from the internal tissues of healthy rice plants. The isolation procedure involved cultivating bacterial samples in chlorpyrifos-enriched minimal salt agar media, a method adapted from previous reports, to select for microorganisms capable of thriving in the presence of this pesticide, as descibed methods [1-4]. Subsequent to isolation, the purified bacterial colonies underwent comprehensive biochemical characterization using a panel of standard tests including catalase, oxidase, citrate utilization, methyl red, Voges-Proskauer, urease, triple sugar iron agar, and indole tests. These tests were conducted strictly according to the guidelines outlined in Bergey's Manual of Systematic Bacteriology to aid in preliminary identification and metabolic profiling [21]. Further assessment of specific enzyme activities, indicative of their metabolic capabilities, was performed by observing the formation of clear zones around bacterial colonies on specific agar plates, following established protocols [22].

2.2. Whole genome sequencing, taxonomy, genome comparison, and gene prediction

The genomic DNA of the bacterial strains was extracted, and genomic libraries were prepared according to standard protocols as described [17]. Whole genome sequencing was performed using the Illumina MiniSeq System, following established methodologies. The quality of the raw sequencing reads and assembled genome sequences was rigorously assessed through FastQC analysis and monitored via the Base Space Illumina sequence analysis Hub. The annotated genome sequence of the three strains constructed into a complete CDS (coding DNA sequences) map our own developed using Linux operating systems method. For taxonomic classification and phylogenetic analysis, housekeeping genes, specifically *rec*A, *gyr*B, *rpo*B, and 16S rRNA, were extracted and analyzed. A robust phylogenetic tree of the strains was constructed with 1000 bootstrap values using MegaXI software. Furthermore, a comprehensive prediction of various functional genes was performed from the PGAP files of the strains. This included genes associated with plant growth-promoting traits (such as N-fixation, P-solubilization, Indole-3-acetic acid and 1-aminocyclopropane-1-carboxylate deaminase production, and sulfur assimilation), biofilm formation, root colonization mechanisms (chemotaxis and motility), abiotic stress tolerance, and the production of antimicrobial peptides [3, 4].

2.3. Pesticide-degrading protein modeling, virtual screening, and docking

2.3a. Protein modeling and structure validation

Three-dimensional (3D) structures of putative pesticide-degrading proteins from *Serratia* sp. HSTU-ABk35 were predicted via homology modeling, utilizing known experimental structures from the Protein Data Bank as templates [3]. Model

generation, including template alignment and structural refinement, was performed using established tools such as I-TASSER [4].

Stereochemical quality was assessed using ERRAT, with scores above 80% indicating good quality [23, 25]. VERIFY-3D evaluated the 3D-1D profile, with scores over 80% confirming high structural integrity (Ramzan et al., 2024). Ramachandran plots analyzed amino acid dihedral angles (phi and psi), ensuring a high percentage of residues in favored regions (e.g., >90%) for model reliability [24, 25].

2.3b. Virtual screening

Virtual screening identified potential pesticide binders against predicted protein models. This structure-based approach involved docking a pesticide library into defined protein active sites as previously described [3, 4]. Pesticide compounds and protein receptors were prepared through 3D structure generation, energy minimization, and format conversion [3, 4, 26]. The screening process employed docking software to predict optimal binding poses and assign binding affinity scores (e.g., Kcal/mol) [23]. This resulted in a ranked list of compounds based on predicted binding energies, facilitating the prioritization of potential interactions.

2.3c. Molecular docking and catalytic interaction analysis

Detailed molecular docking was performed on selected protein-pesticide complexes to elucidate specific molecular interactions [27]. Docking algorithms sampled various ligand conformations within protein binding sites, predicting stable complex structures and binding energies [21, 24]. The analysis focused on identifying key stabilizing interactions, including hydrogen bonds, hydrophobic contacts, and salt bridges. Emphasis was placed on identifying catalytic triads or diads, critical enzymatic motifs, to infer potential degradation mechanisms and roles of specific active site residues [3, 4].

3. RESULTS

3.1. Biochemical characterization of *Serratia* sp. HSTU-ABk35

The biochemical profiling of *Serratia* sp. strain HSTU-ABk35 revealed a broad range of positive enzymatic and metabolic activities (**Table 1**), supporting its taxonomic placement within the genus *Serratia* and highlighting its functional versatility. The isolate tested positive for oxidase, catalase, and citrate utilization, indicating an active aerobic metabolism and the ability to use citrate as a sole carbon source. Positive MIU reactions further suggested motility and indole utilization capacity, while the absence of mortality response confirmed the non-lethal nature of the strain under the tested conditions. The strain exhibited a positive urease reaction, reflecting its potential to hydrolyze urea and contribute to nitrogen cycling. In the IMViC series, *Serratia* sp. HSTU-ABk35 showed a positive Voges–Proskauer (VP) reaction and a negative methyl red (MR) test, indicating a butanediol fermentation pathway rather than mixed-acid fermentation. The triple sugar iron (TSI) test was positive, suggesting efficient carbohydrate utilization without hydrogen sulfide production.

Table 1: Biochemical analyses of *Serratia* sp. HSTU-Abk35.

	Oxidase	Citrate	Catalase	MIU	Mortality	Urease	VP	MR	TSI	Lactose	Sucrose	Dextrose	CMCase	Xylanase	Amylase	Protease
Serratia sp. strain HSTU-ABk35	+	+	+	+	-	+	+	-	+	+	+	+	+	+	+	+

Carbohydrate fermentation assays demonstrated the ability of the strain to metabolize lactose, sucrose, and dextrose, indicating metabolic flexibility toward diverse carbon sources. Notably, the isolate expressed strong extracellular hydrolytic enzyme activities, including CMCase (cellulase), xylanase, amylase, and protease. The presence of these enzymes underscores the strain's capacity to degrade complex polysaccharides and proteins, which may enhance nutrient mobilization and ecological adaptability in plant-associated or soil environments. Overall, the biochemical traits of *Serratia* sp. HSTU-ABk35 reflect a metabolically robust bacterium with multifunctional enzymatic potential.

3.2. Phylogenetic taxonomy of the endophytic bacteria

3.2a. Genome annotation and phylogenetic relationship of the strains

The annotated genome sequence of the three strains revealed a complete CDS (coding DNA sequences) map with genetic repertoire of predicted genes distributed across the genome (**Figure 1**). The genome map of *Serratia* sp. HSTU-ABk35 shows a linear chromosome of 5,346,384 bp with a dense and uniform distribution of coding sequences (CDSs) across both strands. Protein-coding genes are tightly packed throughout the genome, indicating efficient genome organization and high metabolic capacity. The genome of the strain have no large intergenic gaps, indicating strong coding potential. CDSs are evenly distributed on both forward and reverse strands, suggesting balanced transcriptional organization. The genome map shows distinct GC content and GC skew patterns, with localized deviations that may represent functionally specialized or horizontally acquired regions. Numerous CDS clusters are visible across the chromosome, consistent with operon-based gene organization typical of bacteria. The abundance of annotated enzymatic CDSs (e.g., oxidoreductases, hydrolases, transferases) highlights the strain's metabolic versatility and adaptive potential.

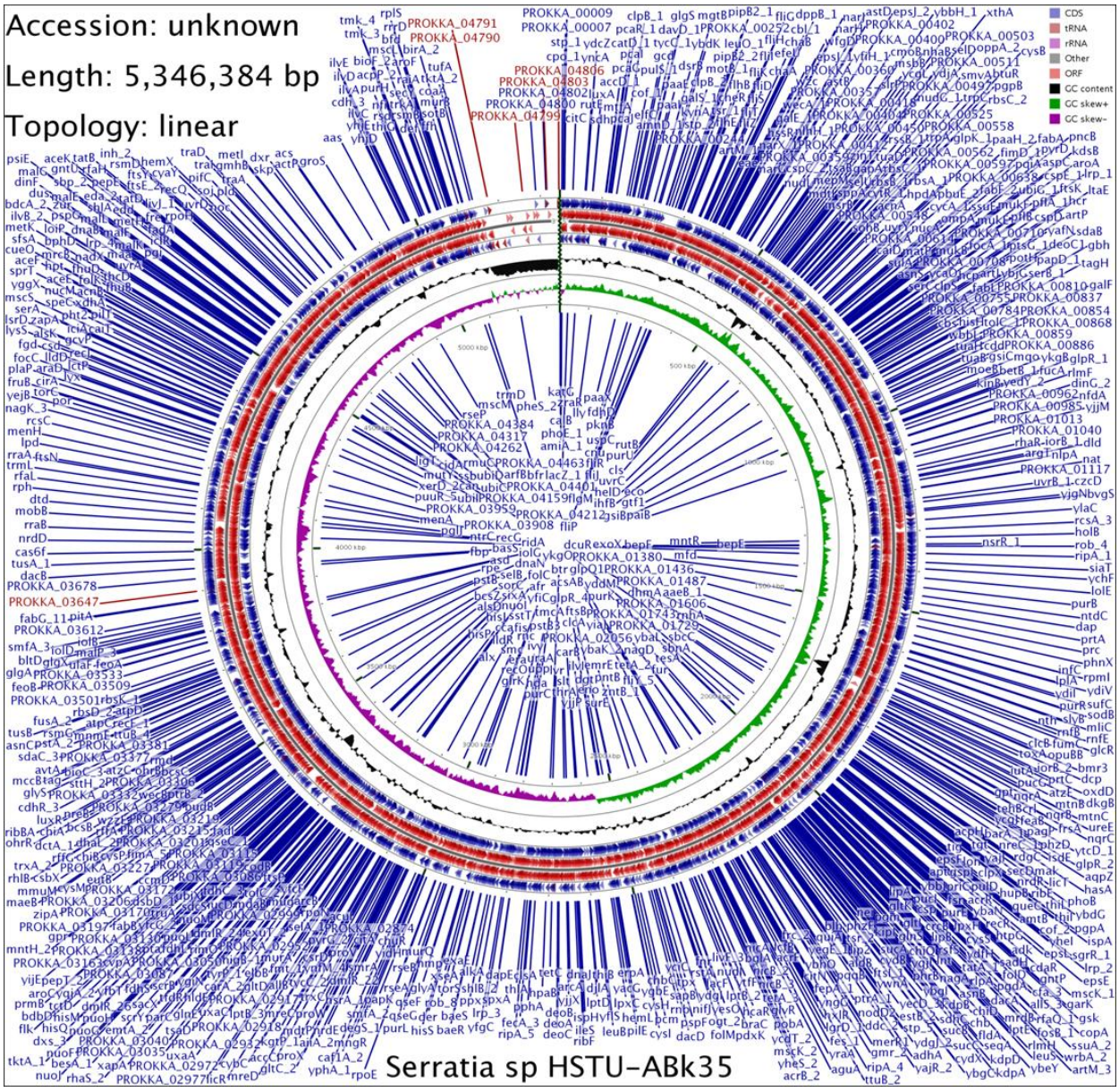

Figure 1. A CDS (coding DNA sequences) map of for *Serratia* sp. strain HSTU-Abk35.

As seen in Figure **2A**, circular plot of the three strains pangenome plot the pink color slot identified as pan-genome and white space indicates a region missing in the specified genome. The circular plot clearly intimate that a several portions of the genome sequence of *Serratia* sp. HSTU-ABk35 were not similar compared with other six closest strains (**Figure 2A**).

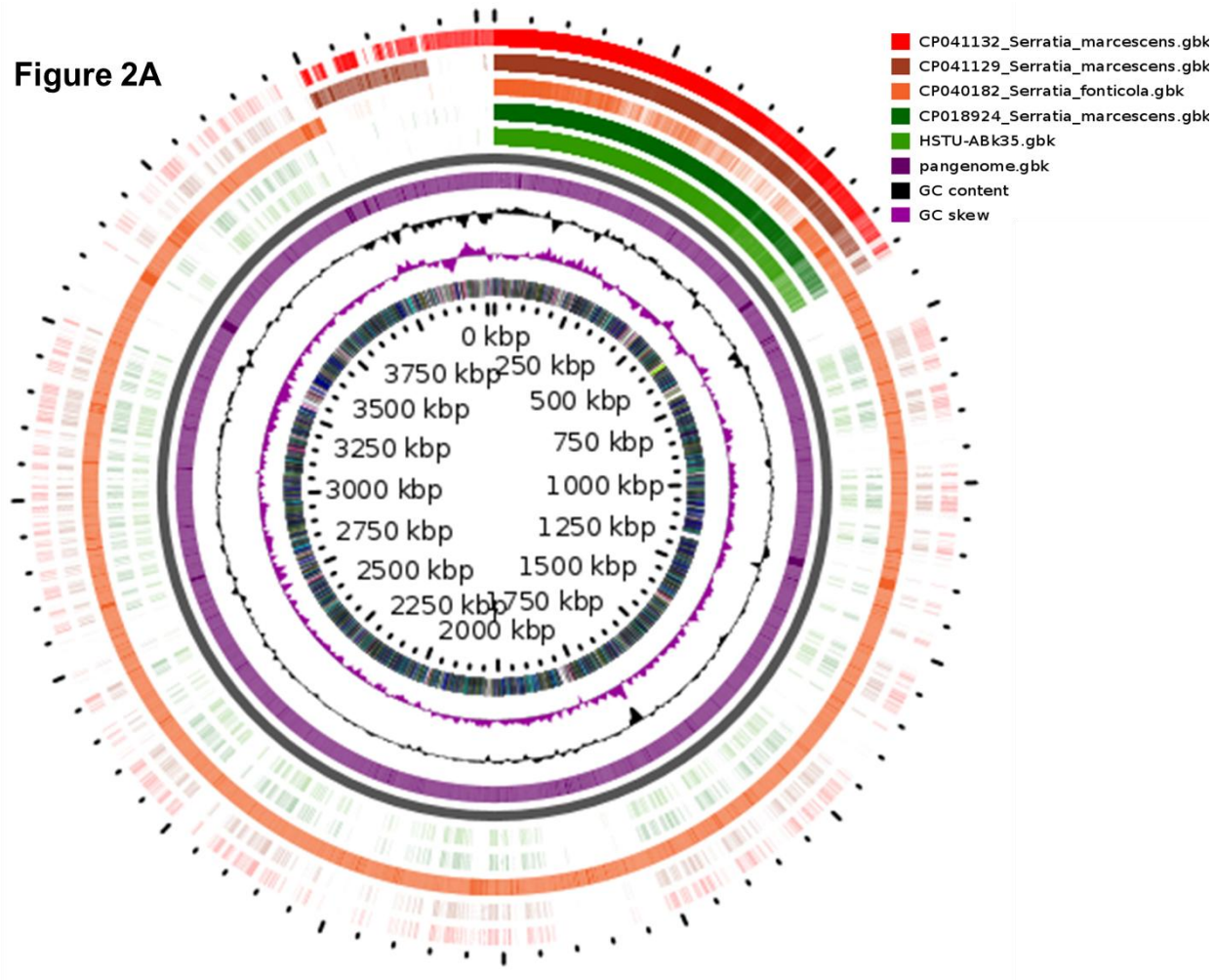

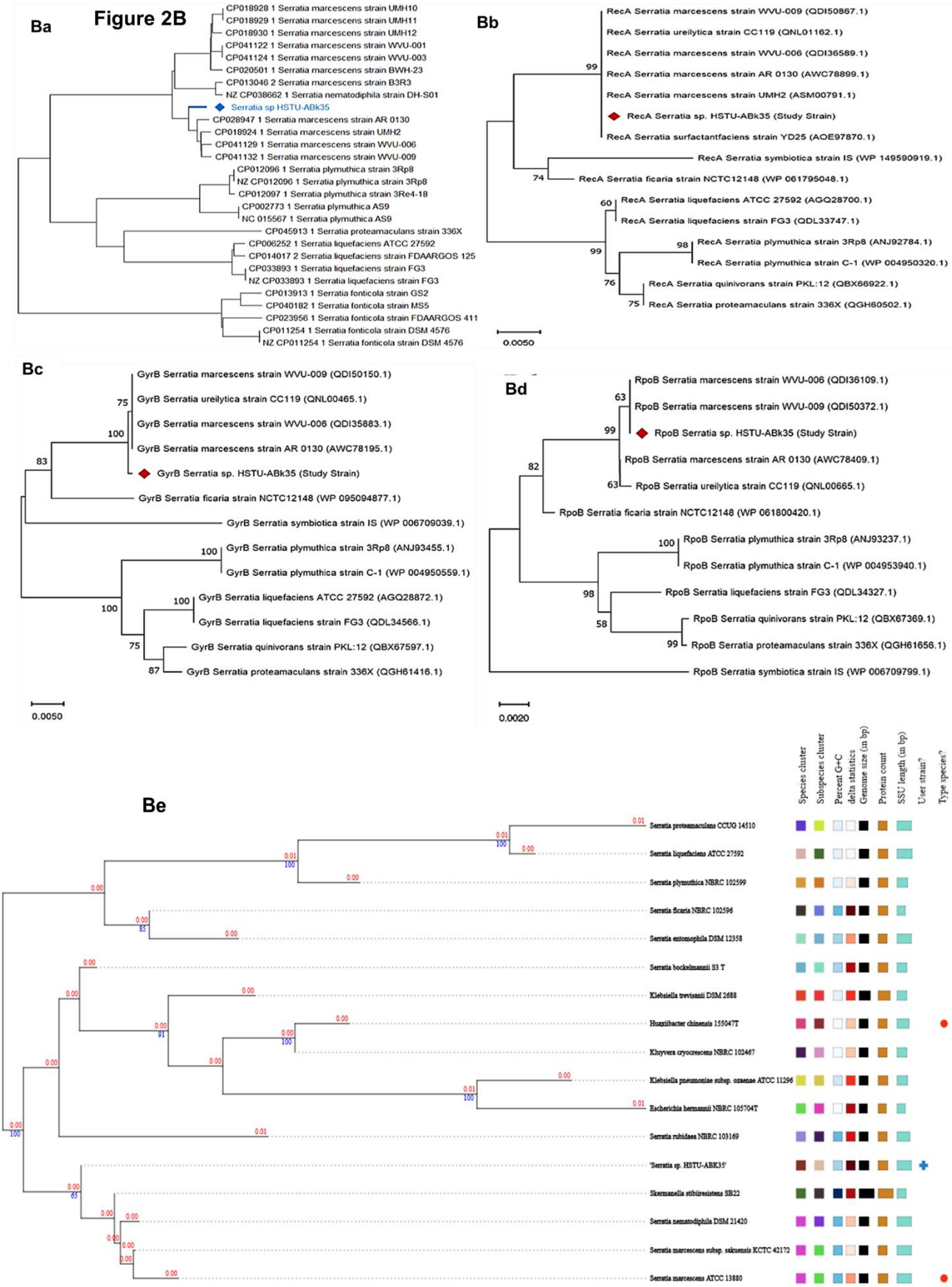
Figure 2B
Ba
CP018928 1 Serratia marcescens strain UMH10
CP018929 1 Serratia marcescens strain UMH11
CP018930 1 Serratia marcescens strain UMH12
CP041122 1 Serratia marcescens strain WVU-001
CP041124 1 Serratia marcescens strain WVU-003
CP020501 1 Serratia marcescens strain BWH-23
CP013046 2 Serratia marcescens strain B3R3
NZ CP038662 1 Serratia nematodiphila strain DH-S01
Serratia sp HSTU-ABk35
CP028947 1 Serratia marcescens strain AR 0130
CP018924 1 Serratia marcescens strain UMH2
CP041129 1 Serratia marcescens strain WVU-006
CP041132 1 Serratia marcescens strain WVU-009
CP012096 1 Serratia plymuthica strain 3Rp8
NZ CP012096 1 Serratia plymuthica strain 3Rp8
CP012097 1 Serratia plymuthica strain 3Re4-18
CP002773 1 Serratia plymuthica AS9
NC 015567 1 Serratia plymuthica AS9
CP045913 1 Serratia proteamaculans strain 336X
CP006252 1 Serratia liquefaciens ATCC 27592
CP014017 2 Serratia liquefaciens strain FDAARGOS 125
CP033893 1 Serratia liquefaciens strain FG3
NZ CP033893 1 Serratia liquefaciens strain FG3
CP013913 1 Serratia fonticola strain GS2
CP040182 1 Serratia fonticola strain MS5
CP023956 1 Serratia fonticola strain FDAARGOS 411
CP011254 1 Serratia fonticola strain DSM 4576
NZ CP011254 1 Serratia fonticola strain DSM 4576
Bb
RecA Serratia marcescens strain WVU-009 (QDI50867.1)
RecA Serratia ureilytica strain CC119 (QNL01162.1)
RecA Serratia marcescens strain WVU-006 (QDI36589.1)
RecA Serratia marcescens strain AR 0130 (AWC78899.1)
RecA Serratia marcescens strain UMH2 (ASM00791.1)
RecA Serratia sp. HSTU-ABk35 (Study Strain)
RecA Serratia surfactantfaciens strain YD25 (AOE97870.1)
RecA Serratia symbiotica strain IS (WP 149590919.1)
RecA Serratia ficaria strain NCTC12148 (WP 061795048.1)
RecA Serratia liquefaciens ATCC 27592 (AGQ28700.1)
RecA Serratia liquefaciens strain FG3 (QDL33747.1)
RecA Serratia plymuthica strain 3Rp8 (ANJ92784.1)
RecA Serratia plymuthica strain C-1 (WP 004950320.1)
RecA Serratia quinivorans strain PKL:12 (QBX66922.1)
RecA Serratia proteamaculans strain 336X (QGH60502.1)
0.0050
Bc
GyrB Serratia marcescens strain WVU-009 (QDI50150.1)
GyrB Serratia ureilytica strain CC119 (QNL00465.1)
GyrB Serratia marcescens strain WVU-006 (QDI35883.1)
GyrB Serratia marcescens strain AR 0130 (AWC78195.1)
GyrB Serratia sp. HSTU-ABk35 (Study Strain)
GyrB Serratia ficaria strain NCTC12148 (WP 095094877.1)
GyrB Serratia symbiotica strain IS (WP 006709039.1)
GyrB Serratia plymuthica strain 3Rp8 (ANJ93455.1)
GyrB Serratia plymuthica strain C-1 (WP 004950559.1)
GyrB Serratia liquefaciens ATCC 27592 (AGQ28872.1)
GyrB Serratia liquefaciens strain FG3 (QDL34566.1)
GyrB Serratia quinivorans strain PKL:12 (QBX67597.1)
GyrB Serratia proteamaculans strain 336X (QGH61416.1)
0.0050
Bd
RpoB Serratia marcescens strain WVU-006 (QDI36109.1)
RpoB Serratia marcescens strain WVU-009 (QDI50372.1)
RpoB Serratia sp. HSTU-ABk35 (Study Strain)
RpoB Serratia marcescens strain AR 0130 (AWC78409.1)
RpoB Serratia ureilytica strain CC119 (QNL00665.1)
RpoB Serratia ficaria strain NCTC12148 (WP 061800420.1)
RpoB Serratia plymuthica strain 3Rp8 (ANJ93237.1)
RpoB Serratia plymuthica strain C-1 (WP 004953940.1)
RpoB Serratia liquefaciens strain FG3 (QDL34327.1)
RpoB Serratia quinivorans strain PKL:12 (QBX67369.1)
RpoB Serratia proteamaculans strain 336X (QGH61656.1)
RpoB Serratia symbiotica strain IS (WP 006709799.1)
0.0020
Be
Species cluster
Subspecies cluster
Percent G+C
delta statistics
Genome size (in bp)
Protein count
SSU length (in bp)
User strain?
Type species?
Serratia proteamaculans CCUG 14510
Serratia liquefaciens ATCC 27592
Serratia plymuthica NBRC 102599
Serratia ficaria NBRC 102596
Serratia entomophila DSM 12358
Serratia bockelmannii S3 T
Klebsiella trevisanii DSM 2688
Huaxiibacter chinensis 155047T
Kluyvera cryocrescens NBRC 102467
Klebsiella pneumoniae subsp. ozaenae ATCC 11296
Escherichia hermannii NBRC 105704T
Serratia rubidaea NBRC 103169
'Serratia sp. HSTU-ABK35'
Skermanella stibiiresistens SB22
Serratia nematodiphila DSM 21420
Serratia marcescens subsp. sakuensis KCTC 42172
Serratia marcescens ATCC 13880

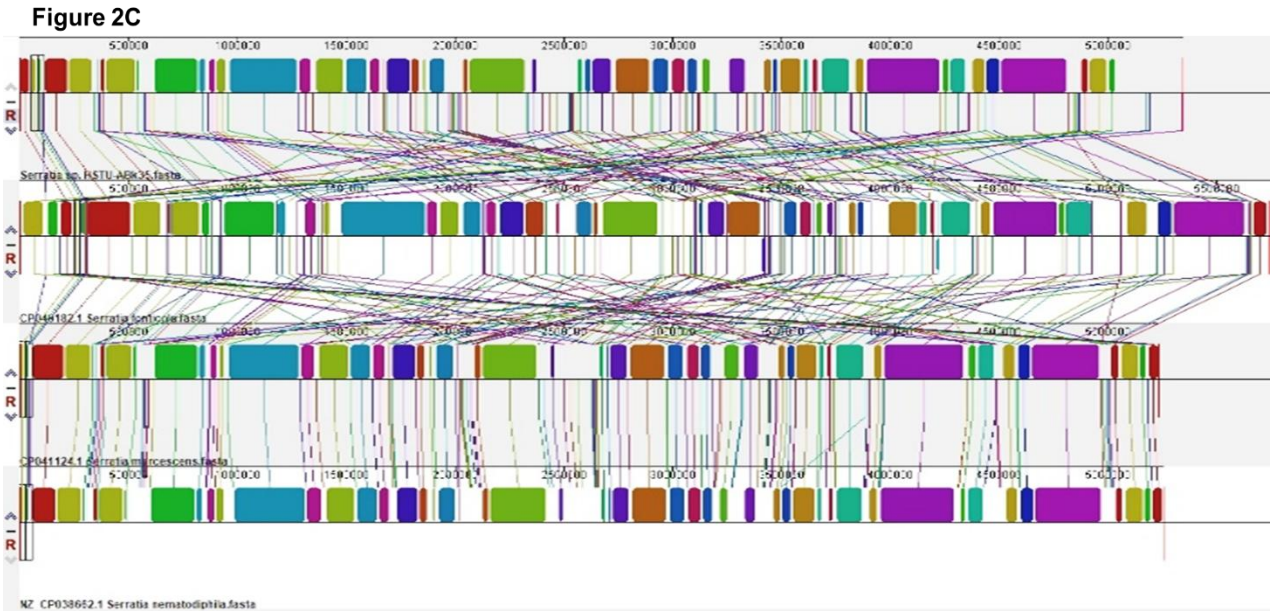

Figure 2. Genome comparison and phylogenetic analysis of the strain *Serratia* sp. HSTU-Abk35**. (A)** Pangenome analysis of the strain. **(B) Phylogeny of the strain,** (**Ba**) Whole genome phylogenetic tree of the strain; (**Bb**) phylogenetic tree based on housekeeping gene *rec*A; (**Bc**) phylogenetic tree based on housekeeping gene *gyr*B; (**Bd**) phylogenetic tree based on housekeeping gene *rpo*B; (**Be**) phylogenetic tree based on housekeeping gene (16S rRNA) analysis of *Serratia* sp. HSTU-ABk35. (**C**) Progressive Mauve alignment (LCBs) of the strain *Serratia* sp. HSTU-ABk35 with their nearest homologs.

The whole genome phylogenetic tree of strain, *Serratia* sp. HSTU-ABk35 showed that it was placed completely in a single node that is originated from two parental node i.e. one node lead by strain, *Serratia marcescens* AR0130 and other node represented by strain, *Serratia nematodiphila* DS-SO1 (**Figure 2Ba**). The pairwise highest ANI blast (ANIb) score of strain, *Serratia* sp. HSTU-ABk35 was hit with *Serratia ureilytica* (CP060276.1) 99.12%, followed by *Serratia marcescens* (CP041132.1) 98.82% (**Table 2a**). Furthermore, the dDDH analysis of strain, *Serratia* sp. HSTU-ABk35 with its nearest homologs strain, *Serratia nematodiphila* DSM21420 showed 77.4% dDDH value, and 0.67% G+C content, followed by strain, *Serratia marcescens* sub sp. *sakuensis* KCTC42172 showed 74.6% dDDH value, and 0.78% G+C content (**Table 2b**), while *rec*A gene of strain, *Serratia* sp. HSTU-ABk35 was placed in the same node with *rec*A gene of strains, *Serratia marcescens* UMH2 and *Serratia ureilytica* CC119 with 99% similarity (**Figure 2Bb**). In addition, *gyr*B gene of strain, *Serratia* sp. HSTU-ABk35 was placed in a separate node from strains, *Serratia marcescens* and *Serratia ficaria* (**Figure 2Bc**) and *rpo*B gene was placed in the same node with strain, *S. marcescens* (**Figure 2Bd**). In addition, the 16S rRNA gene sequence analysis of the strain had shown nearest relationship, but separate cluster, with *Serratia rubidae* (**Figure 2Be**). Therefore, the strain, *Serratia* sp. HSTU-ABk35 might belongs to *Serratia marcescens* with evolutionary history.

Multiple genome alignment analysis was conducted to expand our understanding of the genomic features of *Serratia* sp. HSTU-ABk35 (**Figure 2C**). *Serratia* sp. HSTU-ABk35 strains genome was compared with another four individual nearest strains. Each genome isorganized horizontally with homologous segment outlined as colored rectangles. Each same color

block represents a locally collinear block (LCB) or homologous region shared among genomes. The locally collinear block (LCB) of *Serratia* sp. HSTU-ABk35, genome is not totally meet with locally collinear blocks of genomes taken for genomic comparison. Rearrangement of genomic regions was observed between the two genomes in terms of collinearity. As seen, the study strain shared highest homologous region with *Serratia marcescens* for *Serratia* sp. HSTU-ABk35.

Table 2A. Average nucleotide identity (ANIb) of Serratia sp. strain HSTU-ABk35.

	*Serratia*_sp._HSTU-ABk35	CP006252.1_*Serratia_liquefaciens*	CP012096.1_*Serratia_plymuthica*	CP016948.1_*Serratia_surfactantfaciens*	CP018924.1_*Serratia_marcescens*	CP028947.1_*Serratia_marcescens*	CP033893.1_*Serratia_liquefaciens*	CP038467.1_*Serratia_quinivorans*	CP041129.1_*Serratia_marcescens*	CP041132.1_*Serratia_marcescens*	CP045913.1_*Serratia_proteamaculans*	CP060276.1_*Serratia_ureilytica*	NZ_AP019531.1_*Serratia_symbiotica*	NZ_CP053398.1_*Serratia_plymuthica*	NZ_LT906479.1_*Serratia_ficaria*
*Serratia*_sp._HSTU-ABk35.fasta	*	82.84	83.44	93.61	97.66	97.6	82.85	82.77	97.58	97.67	82.61	97.66	81.37	83.39	85.95
CP006252.1_*Serratia_liquefaciens*	82.81	*	86.13	82.71	82.87	82.87	98.31	87.54	82.9	82.82	87.54	82.88	80.87	86.15	83.39
CP012096.1_*Serratia_plymuthica*	83.42	86.15	*	83.43	83.43	83.48	86.08	86.31	83.47	83.52	86.14	83.56	81.13	98.38	84.6
CP016948.1_*Serratia_surfactantfaciens*	93.69	82.8	83.48	*	93.52	93.6	82.84	82.68	93.51	93.5	82.59	93.66	81.55	83.48	85.75
CP018924.1_*Serratia_marcescens*	97.59	82.91	83.53	93.45	*	98.18	82.96	82.83	98.74	98.82	82.69	98.33	81.33	83.53	85.89
CP028947.1_*Serratia_marcescens*	97.74	83.04	83.63	93.59	98.3	*	82.94	82.8	98.32	98.37	82.73	99.12	81.46	83.62	86.05
CP033893.1_*Serratia_liquefaciens*	82.75	98.2	86.05	82.67	82.81	82.65	*	87.5	82.69	82.67	87.29	82.82	81.13	86.13	83.5
CP038467.1_*Serratia_quinivorans*	82.68	87.59	86.42	82.64	82.79	82.69	87.64	*	82.78	82.78	95.33	82.78	80.93	86.34	83.76
CP041129.1_*Serratia_marcescens*	97.62	82.94	83.61	93.5	98.76	98.2	82.91	82.76	*	99.06	82.67	98.31	81.42	83.6	85.82
CP041132.1_*Serratia_marcescens*	97.7	82.95	83.64	93.48	98.74	98.24	82.88	82.75	99.01	*	82.68	98.36	81.56	83.56	85.84
CP045913.1_*Serratia_proteamaculans*	82.46	87.56	86.25	82.51	82.57	82.54	87.46	95.33	82.56	82.55	*	82.64	80.76	86.21	83.47
CP060276.1_*Serratia_ureilytica*	97.6	82.97	83.64	93.47	98.27	98.94	82.98	82.93	98.19	98.24	82.79	*	81.39	83.68	86.07
NZ_AP019531.1_*Serratia_symbiotica*	82.6	81.73	82.41	82.64	82.52	82.51	81.94	81.87	82.5	82.5	81.71	82.52	*	82.38	83.51
NZ_CP053398.1_*Serratia_plymuthica*	83.38	86.08	98.32	83.48	83.48	83.5	86.17	86.25	83.5	83.47	86.11	83.58	81.29	*	84.4
NZ_LT906479.1_*Serratia_ficaria*	86.39	83.84	85.07	86.39	86.32	86.36	83.92	84.11	86.27	86.28	83.81	86.41	82.65	85	*

Table 2B. Digital DNA–DNA hybridization (dDDH) for species determination of Serratia sp. strain HSTU-ABk35.

Subject strain	dDDH (d0, in %)	C.I. (d0, in %)	dDDH (d4, in %)	C.I. (d4, in %)	dDDH (d6, in %)	C.I. (d6, in %)	G+C content difference (in %)
Serratia nematodiphila DSM 21420	77.6	[73.6 -81.1]	63.0	[60.1 -65.8]	77.4	[73.9 -80.5]	0.67
Serratia marcescens subsp. sakuensis KCTC42172	74.5	[70.5 -78.1]	62.3	[59.4 -65.1]	74.6	[71.1 -77.7]	0.78
Serratia marcescens ATCC 13880	75.7	[71.7 -79.3]	61.5	[58.6 -64.3]	75.4	[71.9 -78.5]	0.97
Serratia bockelmanniiS3 T	70.8	[66.9 -74.5]	61.2	[58.4 -64.0]	71.2	[67.7 -74.4]	0.18
Serratia ficaria NBRC102596	56.1	[52.6 -59.6]	34.3	[31.9 -36.9]	50.5	[47.5 -53.6]	1.04
Serratia entomophilaDSM 12358	58.6	[54.9 -62.1]	33.4	[31.0 -35.9]	51.9	[48.9 -55.0]	0.05
Serratia plymuthicaNBRC 102599	45.7	[42.3 -49.1]	28.1	[25.7 -30.6]	40.3	[37.3 -43.3]	2.91
Serratia liquefaciensATCC 27592	48.7	[45.3 -52.2]	27.1	[24.7 -29.5]	42.0	[39.0 -45.0]	3.54
Serratia proteamaculansCCUG 14510	47.2	[43.8 -50.7]	26.9	[24.5 -29.4]	40.9	[37.9 -43.9]	3.74
Serratia rubidaea NBRC103169	36.5	[33.1 -40.0]	26.4	[24.1 -28.9]	33.0	[30.1 -36.1]	0.43
Skermanella stibiiresistens SB22	12.6	[9.9 -15.8]	23.7	[21.4 -26.2]	13.0	[10.7 -15.7]	6.99
Klebsiella pneumoniaesubsp. ozaenae ATCC 11296	17.1	[14.1 -20.7]	20.7	[18.5 -23.1]	17.0	[14.4 -19.9]	1.61
Klebsiella trevisanii DSM2688	15.5	[12.6 -19.0]	20.7	[18.5 -23.1]	15.6	[13.1 -18.5]	3.72
Escherichia hermanniiNBRC 105704T	15.5	[12.6 -19.0]	20.4	[18.2 -22.8]	15.5	[13.0 -18.4]	4.8
Huaxiibacter chinensis155047T	15.1	[12.2 -18.5]	20.2	[18.0 -22.6]	15.2	[12.7 -18.1]	5.16
Kluyvera cryocrescens NBRC 102467	15.5	[12.6 -19.0]	20.1	[17.9 -22.5]	15.6	[13.0 -18.5]	5.02

3.2b. Plant growth promoting genes of pesticide degrading endophytic bacteria

The assembled genome of the respective strains, *Serratia* sp. HSTU-Abk35 (**Table 3a**) encoded a number of nitrogen-fixing, nitrosative stress, and nitrogen metabolism regulatory proteins, including *isc*U, nifJS, nsrR, glnK, glnD, and ptsN . In particular, the strains possessed the genes encoding nitrate reductase, nitrite reductase, and associated transporters, ACC-deaminase, superoxide dismutase, high-affinity siderophore (enterobactin), IAA producing enzyme, phosphate and trehalose metabolic enzymes, sulfur and ammonia assimilatory, and biofilm forming. The assembled genome of these three strains revealed the presence of root-colonizing genes. In addition, the genome *Serratia* sp. HSTU-Abk35 contained annotated systemic resistance inducer genes, including VOCs (volatile compounds) genes, and synthetic genes, such as methanethiol (*met*H), 2,3-butanediol (*ilv*BNACYDM), isoprene (*gcp*E/*isp*G, *isp*E), acetolactate decarboxylase (*bud*A), spermidine synthesis (*spe*EABD), and oxidoreductase and hydrolase (*amy*A) genes. A set of antimicrobial peptide synthesis genes, such as *pag*P, *sap*BC, *lip*A, *lip*B, and *amy*A genes, was observed in the annotated genome (**Table 3a**).

Table 3A. Genes associated with plant growth promotion (PGP) available in genome *Serratia* sp. HSTU-ABk35.

PGP activities description		Gene annotation	Chromosome location	Locus Tag	E.C. number
Nitrogen fixation	nifJ	Pyruvate: ferredoxin (flavodoxin) oxidoreductase	292050..295583	GPJ58_11545	-
	nifS	cysteine desulfurase	135906..137120	GPJ58_13915	2.8.1.7
	iscU	Fe-S cluster assembly scaffold	135495..135881	GPJ58_13910	-
Nitrosative stress	nsrR	Nitric oxide sensing transcriptional repressor	14192..14617	GPJ58_18580	-
	glnK	P-II family nitrogen regulator	196845..197183	GPJ58_09290	-
nitrate reductase,	-	nitrate reductase subunit alpha	GPJ58_01815	GPJ58_01815	1.7.99.4
nitrite reductase, and	*nar*H	nitrate reductase subunit beta	407283..408827	GPJ58_01820	1.7.99.4
associated transporters	*nar*J	nitrate reductase molybdenum cofactor assembly chaperone	408824..409546	GPJ58_01825	-
	*nar*I	respiratory nitrate reductase subunit gamma	409549..410226	GPJ58_01830	1.7.99.4
	-	nitrate reductase	155594..156142	GPJ58_16505	-

	*Nir*D	nitrite reductase small subunit NirD	39471..39797	GPJ58_17880	-
	-	nitrate reductase subunit alpha	149433..151118	GPJ58_16480	1.7.99.4
Acetolactate decarboxylase	*bud*A	Acetolactate decarboxylase	151151..151930	GPJ58_16485	4.1.1.5
Nitrogen metabolism regulatory protein	glnD	Bifunctional uridylyl removing protein	42171..44834	GPJ58_22755	2.7.7.59
	glnB	Nitrogen regulatory protein P-II	158223..158561	GPJ58_14010	-
	ptsN	Nitrogen regulatory protein PtsN	62566..63012	GPJ58_15005	-
Ammonia assimilation	gltB	glutamate synthase large subunit	83748..88208	GPJ58_15135	1.4.1.13
	gltS	sodium/glutamate symporter	24791..26002	GPJ58_19400	
	amtB	Ammonium transporter AmtB	197219..198505	GPJ58_09295	-
ACC deaminase	dcyD	D-cysteine desulfhydrase	350129..351121	GPJ58_01600	4.4.1.15
	rimM	ribosome maturation factor RimM	13791..14339	GPJ58_11820	-
Siderophore					
Siderophore enterobactin	fes	enterochelin esterase	125919..127181	GPJ58_10850	3.1.1.-
	entC	isochorismate synthase EntC	29818..31023	GPJ58_22940	5.4.4.2
	entS	enterobactin transporter EntS	115761..117044	GPJ58_10835	-
	entE	2,3-dihydroxybenzoyl)adenylate synthase	31031..32659	GPJ58_22945	2.7.7.58
	fhuA	ferrichrome porin FhuA	64477..66669	GPJ58_21180	-
	fhuB	Fe (3^+)-hydroxamate ABC transporter permease FhuB	68419..70407	GPJ58_21195	-
	fhuC	$Fe3^+$-hydroxamate ABC transporter ATP-binding protein	66717..67514	GPJ58_21185	-
	fhuD	Fe (3^+)-hydroxamate ABC transporter substrate-binding protein	67514..68422	GPJ58_21190	-
	tonB	TonB system transport protein TonB	603377..604120	GPJ58_02810	-
	fepB	$Fe2^+$-enterobactin ABC transporter substrate-binding protein	143531..144538	GPJ58_16455	-
	fepG	iron-enterobactin ABC transporter permease	145809..146846	GPJ58_16465	-
	exbD	TonB system transport protein ExbD	191384..191806	GPJ58_15620	-
	rpoA	DNA-directed RNA polymerase subunit alpha	11203..12192	GPJ58_23825	2.7.7.6
	rpoB	DNA-directed RNA polymerase subunit beta	4163..8191	GPJ58_23520	2.7.7.6
	exbB	tol-pal system-associated acyl-CoA thioesterase	190403..191380	GPJ58_15615	-
Plant hormones					
IAA production	trpCF	bifunctional indole-3-glycerol-phosphate synthase TrpC	611973..613334	GPJ58_02860	4.1.1.48/5.3.1.24
	trpS	tryptophan--tRNA ligase	462106..463113	GPJ58_05220	6.1.1.2
	trpA	tryptophan synthase subunit alpha	609935..610741	GPJ58_02850	4.2.1.20
	trpD	bifunctional anthranilate synthase glutamate amido transferase component	613338..614336	GPJ58_02865	2.4.2.18/4.1.3.27
Phosphate metabolism	pitA	inorganic phosphate transporter PitA	170376..171878	GPJ58_18405	-
	pstS	phosphate ABC transporter substrate-binding protein PstS	171797..172837	GPJ58_17535	-
	pstC	phosphate ABC transporter permease PstC	170749..171705	GPJ58_17530	-
	pstA	phosphate ABC transporter permease PstA	169857..170747	GPJ58_17525	-
	pstB	phosphate ABC transporter ATP-binding protein PstB	169032..169808	GPJ58_17520	-
	phoU	phosphate signaling complex protein PhoU	168286..169020	GPJ58_17515	3.5.2.6
	ugpB	sn-glycerol-3-phosphate ABC transporter substrate-binding protein UgpB	34307..35626	GPJ58_21855	--
	ugpE	sn-glycerol-3-phosphate ABC transporter substrate-binding protein UgpE	32499..33344	GPJ58_21845	-
	phoA	alkaline phosphatase	328821..330248	GPJ58_04570	3.1.3.1
	phoB	phosphate response regulator transcription factor PhoB	135120..135809	GPJ58_09005	-
	phoR	phosphate regulon sensor histidine kinase PhoR	135834..137150	GPJ58_09010	2.7.13.3
	ppx	exopolyphosphatase	54567..56117	GPJ58_13560	3.6.1.11
	ppk1	polyphosphate kinase 1	52493..54556	GPJ58_13555	2.7.4.1
	phoH	phosphate starvation-inducible protein PhoH	364084..364872	GPJ58_01645	-
	pntA	Re/Si-specific NAD(P)(+) transhydrogenase subunit alpha	267170..268699	GPJ58_11430	1.6.1.2
	pntB	Re/Si-specific NAD(P)(+) transhydrogenase subunit beta"	265765..267159	GPJ58_11425	-
	phoQ	two-component system sensor histidine kinase PhoQ	171572..173029	GPJ58_06810	2.7.13.3
Biofilm formation	tomB	Hha toxicity modulator TomB	216969..217337	GPJ58_09415	-
	luxS	S-ribosylhomocysteine lyase	18539..19054	GPJ58_11845	4.4.1.21

	murJ	Murein biosynthesis integral membrane protein MurJ	477332..478867	GPJ58_02200	-
	flgH	Flagellar basal body L-ring protein FlgH	320491..321192	GPJ58_01450	-
	flgJ	Flagellar assembly peptidoglycan hydrolase FlgJ	322303..323247	GPJ58_01460	3.2.1.-
	flgL	Flagellar hook-filament junction protein FlgL	325163..326122	GPJ58_01470	-
	flgM	Flagellar biosynthesis anti-sigma factor FlgM	314793..315104	GPJ58_01410	-
	flgA	Flagellar basal body P-ring formation protein	315233..315886	GPJ58_01415	-
	flgB	Flagellar basal body rod protein FlgB	316047..316460	GPJ58_01420	-
	flgI	Flagellar basal body P-ring protein FlgI	321203..322303	GPJ58_01455	-
	flgG	Flagellar basal-body rod protein FlgG	319625..320407	GPJ58_01445	-
	motA	Flagellar motor stator protein MotA	297739..298629	GPJ58_01320	-
	motB	Flagellar motor protein MotB	298626..299690	GPJ58_01325	-
	efp	elongation factor P	52848..53414	GPJ58_23055	-
	hfq	RNA chaperone Hfq	8280..8588	GPJ58_18550	-
Sulfur assimilation and metabolism	cysZ	sulfate transporter CysZ	162264..163022	GPJ58_16540	-
	cysK	cysteine synthase A	163208..164176	GPJ58_16545	2.5.1.47
	cysM	cysteine synthase CysM	169505..170386	GPJ58_16575	2.5.1.47
	cysA	sulfate/thiosulfate ABC transporter ATP-binding protein CysA	170468..171556	GPJ58_16580	-
	cysW	sulfate/thiosulfate ABC transporter permease CysW"	171546..172421	GPJ58_16585	-
	cysC	adenylyl-sulfate kinase	47986..48675	GPJ58_12010	2.7.1.25
	cysN	sulfate adenylyl transferase subunit CysN	48614..50041	GPJ58_12015	2.7.7.4
	cysD	sulfate adenylyl transferase subunit CysD	50053..50961	GPJ58_12020	2.7.7.4
	cysH	Phosphor adenosine phosphosulfate reductase	53802..54536	GPJ58_12035	1.8.4.8
	cysI	assimilatory sulfite reductase (NADPH)	54598..56313	GPJ58_12040	1.8.1.2
	cysJ	NADPH-dependent assimilatory sulfite reductase flavoprotein subunit	56313..58112	GPJ58_12045	1.8.1.2
	cysT	sulfate/thiosulfate ABC transporter permease CysT	172421..173260	GPJ58_16590	-
	cysE	serine O-acetyltransferase	70866..71687	GPJ58_19635	2.3.1.30
	cysQ	3'(2'),5'-bisphosphate nucleotidase CysQ	28840..29583	GPJ58_18675	3.1.3.7
	cysK	cysteine synthase A	163208..164176	GPJ58_16545	2.5.1.47
	cysS	cysteine--tRNA ligase	270209..271594	GPJ58_09655	6.1.1.16
	fdxH	formate dehydrogenase subunit beta	96369..97271	GPJ58_17185	-
Antimicrobial peptide	pagP	lipid IV(A) palmitoyltransferase PagP	81959..82549	GPJ58_08735	2.3.1.251
	sapC	peptide ABC transporter permease SapC	318687..319577	GPJ58_11670	-
	sapB	peptide ABC transporter permease SapB	317735..318700	GPJ58_11665	-
Antibiotic	lipA	lipoyl synthase	305309..306274	GPJ58_09830	2.8.1.8
	lipB	lipoyl(octanoyl) transferase LipB	306267..306926	GPJ58_09835	2.3.1.181
	amyA	alpha-amylase	478286..479776	GPJ58_05310	3.2.1.1
Synthesis of resistance inducers					
Methanethiol	metH	methionine synthase	75928..79623	GPJ58_21630	2.1.1.13
2,3-butanediol	ilvB	acetolactate synthase large subunit	143775..145469	GPJ58_12420	-
	ilvN	acetolactate synthase small subunit	145473..145766	GPJ58_12425	2.2.1.6
	ilvA	Serine, threonine dehydratase	20005..21549	GPJ58_23430	4.3.1.19
	ilvC	ketol-acid reductoisomerase	16151..17626	GPJ58_23410	1.1.1.86
	ilvY	HTH-type transcriptional activator IlvY	17795..18685	GPJ58_23415	-
	ilvD	Dihydroxy-acid dehydratase	21555..23405	GPJ58_23435	4.2.1.9
	ilvM	acetolactate synthase 2 small subunits	24463..24720	GPJ58_23445	2.2.1.6
isoprene	gcpE/ ispG	flavodoxin-dependent (E)-4-hydroxy-3-methylbut-2-enyl-diphosphate synthase	124638..125759	GPJ58_13850	1.17.7.1
	ispE	4-(cytidine 5'-diphospho)-2-C-methyl-D-erythritol kinase	138070..138936	GPJ58_06655	2.7.1.148
acetolactate decarboxylase	*bud*A	acetolactate decarboxylase	151151..151930	GPJ58_16485	4.1.1.5
spermidine synthesis	*spe*E	Polyamine aminopropyltransferase	41546..42409	GPJ58_21075	2.5.1.16
	*spe*A	biosynthetic arginine decarboxylase	73053..75029	GPJ58_21215	4.1.1.19
	*spe*B	agmatinase	75224..76144	GPJ58_21220	3.5.3.11
	*spe*D	adenosylmethionine decarboxylase	40724..41518	GPJ58_21070	4.1.1.50
Symbiosis-related	pyrC	dihydroorotase	42200..43246	GPJ58_06120	3.5.2.3
	gcvT	glycine cleavage system aminomethyltransferase	63760..64857	GPJ58_20715	2.1.2.10
	phnC	phosphonate ABC transporter ATP-binding protein	461155..461988	GPJ58_05215	-
	tatA	Sec-independent protein translocase subunit TatA	16209..16472	GPJ58_21765	-

	zur	Transcriptional repressor /zinc uptake transcriptional repressor	32707..33219	GPJ58_21465	-
Oxidoreductase	sodB	superoxide dismutase [Fe]	353029..353607	GPJ58_07710	1.15.1.1
	gpx	glutathione peroxidase	302928..303479	GPJ58_07465	1.11.1.9
	osmC	peroxiredoxin OsmC	147889..148491	GPJ58_09060	1.11.1.15
Hydrolase	ribA	GTP cyclohydrolase II	70027..70650	GPJ58_17050	3.5.4.25
	folE	GTP cyclohydrolase I FolE	304605..305270	GPJ58_04430	3.5.4.16
	bglF	PTS beta-glucoside transporter subunit IIABC	62500..64365	GPJ58_17020	
	bglX	beta-glucosidase BglX	497320..499617	GPJ58_05410	3.2.1.21
	malZ	maltodextrin glucosidase	144010..145833	GPJ58_09050	3.2.1.20
	bglA	6-phospho-beta-glucosidase	166494..167930	GPJ58_11005	3.2.1.86
	gdhA	NADP-specific glutamate dehydrogenase	175414..176757	GPJ58_18430	1.4.1.4
	-	cellulase	31860..32972	GPJ58_16885	3.2.1.4
	amyA	alpha-amylase	478286..479776	GPJ58_05310	3.2.1.1
Root colonization					
Chemotaxis	malE	maltose/maltodextrin ABC transporter substrate-binding protein	49069..50262	GPJ58_21540	-
	cheY	Two-component system response regulator/ chemotaxis protein CheY	307861..308250	GPJ58_01360	-
	cheB	chemotaxis-specific protein-glutamate methyltransferase CheB	306709..307758	GPJ58_01355	3.1.1.61
	cheW	chemotaxis protein CheW	301741..302241	GPJ58_01335	-
	cheA	chemotaxis protein CheA	299687..301708	GPJ58_01330	-
	rbsB	ribose ABC transporter substrate-binding protein RbsB	197755..198642	GPJ58_17650	-
Motility	flhA	flagellar biosynthesis protein FlhA	310933..313011	GPJ58_01385	-
	flhB	flagellar type III secretion system protein	309789..310940	GPJ58_01380	-
	flhC	Transcriptional activator FlhC/ flagellar transcriptional regulator	297012..297593	GPJ58_01315	-
	flhD	flagellar transcriptional regulator FlhD	296650..297009	GPJ58_01310	-
	fliZ	flagella biosynthesis regulatory protein FliZ	349495..350004	GPJ58_01595	-
	fliD	Flagellar filament capping protein FliD	345803..347203	GPJ58_01580	-
	fliS	flagellar export chaperone Proein	345366..345776	GPJ58_01575	-
	fliE	flagellar hook-basal body complex protein FliE	337952..338266	GPJ58_01540	-
	fliF	flagellar basal body M-ring protein FliF	335942..337636	GPJ58_01535	-
	fliG	flagellar motor switch protein FliG	334953..335945	GPJ58_01530	-
	fliT	flagella biosynthesis regulatory protein FliT	344998..345366	GPJ58_01570	
	fliH	flagellar assembly protein FliH	334256..334960	GPJ58_01525	-
	fliL	flagellar basal body-associated protein FliL	330545..331030	GPJ58_01505	-
	fliM	flagellar motor switch protein FliM	329535..330539	GPJ58_01500	-
	fliP	Flagellar biosynthetic protein FliP/flagellar type III secretion system pore protein	327964..328725	GPJ58_01485	-
	fliQ	flagellar biosynthesis protein FliQ	327673..327942	GPJ58_01480	-
Adhesive structure	hofC	protein transport protein HofC	94559..95758	GPJ58_12200	-
Superoxide dismutase	sodA	superoxide dismutase [Mn]	100759..101379	GPJ58_17195	1.15.1.1
	sodB	superoxide dismutase [Fe]	353029..353607	GPJ58_07710	1.15.1.1
	sodC	superoxide dismutase [Cu-Zn] SodC2	365763..366284	GPJ58_07775	1.15.1.1
Trehalose metabolism	treB	PTS trehalose transporter subunit IIBC	123354..124769	GPJ58_19125	2.7.1.201
	treR	HTH-type transcriptional regulator TreR	124907..125854	GPJ58_19130	
	lamB	maltoporin LamB	45316..46608	GPJ58_21525	-

Analyses of the genomes of these three endophytic bacteria revealed a set of drought resistance, heat shock and cold shock genes (**Table 3A**). Interestingly, the endophytes *Serratia* sp. HSTU-Abk35 were found to have enormous set of genes, including *cha*AB, *pro*ABQVWXPS, *bet*AB, *trk*AH, *kdb*D, and *kdp*ABCE, conferring drought resistance toward host plants (**Table 3**B). Moreover, a set of genes responsible for heavy metals such as arsenic, chromium, and cadmium bioremediation were annotated in the strain's genome. The genomes shelter enormous amount of genes whose products are responsible for pesticide degradation for instance *amp*D, *glp*ABQ, *pde*HR, *pep*ABDE, *phn*FDGHKLMP., carboxylesterase family protein, amidohydrolase, amidohydrolase family protein, α/β-fold hydrolase, and *paa*C (**Table 3C**).

Table 3B. Genes associated with abiotic stress tolerance available in genome *Serratia* sp. HSTU-ABk35.

Activity description	Gene Name	Gene annotation	Chromosome location	Locus Tag	E.C. number
Cold Shock protein	*cspE*	transcription antiterminator/RNA stability regulator CspE	300326..300535	GPJ58_09795	-
	cspD	cold shock-like protein CspD	147230..147451	GPJ58_03730	-
Heat Shock protein	*smpB*	SsrA-binding protein SmpB	201215..201697	GPJ58_14210	-
	hslR	ribosome-associated heat shock protein Hsp15	57973..58380	GPJ58_17970	
	ibpA	heat shock chaperone IbpA	140535..140948	GPJ58_17375	-
	ibpB	heat shock chaperone IbpB	140000..140428	GPJ58_17370	-
	hspQ	heat shock protein HspQ	49462..49779	GPJ58_03340	-
	groL	chaperonin GroEL	47334..47627	GPJ58_23035	-
	groES	Heat shock protein 60 family co-chaperone GroES	47334..47627	GPJ58_23030	-
	yegD	Putative heat shock protein YegD	63748..65100	GPJ58_13590	
	dnaJ	molecular chaperone DnaJ	187704..188828	GPJ58_12600	-
	dnaK	molecular chaperone DnaK	188935..190848	GPJ58_12605	-
	djlA	co-chaperone DjlA	154104..156464	GPJ58_12450	
	rpoH	RNA polymerase sigma factor RpoH	46212..47069	GPJ58_21905	-
	lepA	elongation factor 4	182995..184794	GPJ58_14115	3.6.5.n1
	grpE	nucleotide exchange factor GrpE	196309..196893	GPJ58_14180	-
Heavy metal resistance					
	arsB	arsenical efflux pump membrane protein ArsB	238018..239307	GPJ58_01040	-
	arsC	arsenate reductase (glutaredoxin)	239322..239753	GPJ58_01045	1.20.4.1
	acrR	ultidrug efflux transporter transcriptional repressor AcrR	225916..226575	GPJ58_09460	-
	acrD	Multidrug efflux RND transporter permease	4110..7244	GPJ58_13330	-
	trkA	Trk system potassium transporter TrkA	7549..8925	GPJ58_23795	-
Magnesium transport	*corA*	magnesium/cobalt transporter CorA	75701..76651	GPJ58_22055	-
	corC	CNNM family magnesium/cobalt transport protein CorC	326702..327580	GPJ58_09935	-
	cobA	uroporphyrinogen-III C-methyltransferase	50984..52414	GPJ58_12025	2.1.1.107
Copper homeostasis	*copA*	copper-exporting P-type ATPase CopA	255232..257943	GPJ58_09585	-
	copD	copper homeostasis membrane protein CopD	347230..348102/94013..94894	GPJ58_06400	-
Zinc homeostasis	*znuA*	zinc ABC transporter substrate-binding protein ZnuA	503654..504598	GPJ58_02320	-
	znuB	zinc ABC transporter permease subunit ZnuB	502035..502820	GPJ58_02310	-
	znuC	zinc ABC transporter ATP-binding protein ZnuC	502817..503575	GPJ58_02315	-
Zinc, cadmium, lead and mercury homeostasis					
Zinc homeostasis	*adhP*	alcohol dehydrogenase AdhP	36440..37456	GPJ58_10515	1.1.1.1
	htpX	protease HtpX	261841..262719	GPJ58_07260	3.4.24.-
	zntB	zinc transporter ZntB	297515..298498	GPJ58_11560	-
Manganese homeostasis	*mntR*	manganese-binding transcriptional regulator MntR	62165..62635	GPJ58_06220	-
	mntP	manganese efflux pump MntP	451843..452412	GPJ58_02070	-
	mntH	Mn(2+) uptake NRAMP transporter MntH	62865..64169	GPJ58_06225	-
	nhaA	Na+/H+ antiporter NhaA	186301..187467	GPJ58_12595	-

Drought resistance	*chaA*	sodium-potassium/proton antiporter ChaA	366046..367149	GPJ58_01655	-
	chaB	putative cation transport regulator ChaB	368391..368618	GPJ58_01665	-
	proA	glutamate-5-semialdehyde dehydrogenase	57632..58891	GPJ58_08605	1.2.1.41
	proB	glutamate 5-kinase	56525..57628	GPJ58_08600	2.7.2.11
	proQ	RNA chaperone ProQ	252783..253493	GPJ58_07220	-
	proV	glycine betaine/L-proline ABC transporter ATP-binding protein	277704..278906	GPJ58_14625	-
	proW	glycine betaine/L-proline ABC transporterpermease ProW	278899..280005	GPJ58_14630	-
	proX	glycine betaine/L-proline ABC transporter substrate-binding protein ProX	280075..281076	GPJ58_14635	-
	proP	glycine betaine/L-proline transporter ProP	8027..9529	GPJ58_05945	-
	proS	proline--tRNA ligase	4908..6626	GPJ58_22590	6.1.1.15
	betA	choline dehydrogenase	341752..343419	GPJ58_04620	1.1.99.1
	betB	betaine-aldehyde dehydrogenase	343557..345029	GPJ58_04625	1.2.1.8
	trkA	Trk system potassium transporter TrkA	7549..8925	GPJ58_23795	-
	trkH	Trk system potassium transporter TrkH	656..2107	GPJ58_21695	-
	kdbD	two-component system sensor histidine kinase KdbD	357875..360571	GPJ58_10090	2.7.13.3
	kdpA	potassium-transporting ATPase subunit KdpA	363329..365017	GPJ58_10105	-
	*kdp*B	potassium-transporting ATPase subunit KdpB	361233..363302	GPJ58_10100	-
	*kdp*C	potassium-transporting ATPase subunit KdpC	360645..361214	GPJ58_10095	-
	*kdp*E	/two-component system response regulator KdpE	357169..357858	GPJ58_10085	-

Table 3C. Genes associated with pesticide degradation available in genome *Serratia* sp. HSTU-ABk35.

Activity description	Gene Name	Gene annotation	Chromosome location	Locus Tag	E.C. number
Pesticide degrading	*amp*D	1,6-anhydro-N-acetylmuramyl-L-alanineamidase	90916..91512	GPJ58_12180	3.5.1.28
	*glp*A	anaerobic glycerol-3-phosphate dehydrogenase subunit	64191..65840	GPJ58_22005	1.1.5.3
	*glp*B	glycerol-3-phosphate dehydrogenase subunit	62933..64201	GPJ58_22000	1.1.5.3
	*glp*Q	Glycerol phosphodiester phosphodiesterase	67640..68719	GPJ58_22015	3.1.4.46
	*pep*A	leucyl aminopeptidase	148575..150086	GPJ58_19220	3.4.11.1
	*pep*B	aminopeptidase PepB	130560..131840	GPJ58_13880	3.4.11.23
	*pep*D	cytosol nonspecific dipeptidase	52301..53761	GPJ58_08580	3.4.13.18
	*pep*E	-/dipeptidase PepE	11487..12212	GPJ58_21735	3.4.13.21
	*phn*F	phosphonate metabolism transcriptional regulator PhnF	111772..112497	GPJ58_19070	-
	*phn*D	phosphonate ABC transporter substrate-binding protein	460181..461113	GPJ58_05210	-
	*phn*G	phosphonate C-P lyase system protein PhnG	111328..111771	GPJ58_19065	-
	*phn*H	phosphonate C-P lyase system protein PhnH	110743..111324	GPJ58_19060	2.7.8.37
	*phn*K	phosphonate C-P lyase system protein PhnK	108017..108805	GPJ58_19045	-
	*phn*L	phosphonate C-P lyase system protein PhnL	107305..108000	GPJ58_19040	-
	*phn*M	lpha-D-ribose 1-methylphosphonate 5 triphosphatediphosphatase	113413..114549/106169. 107305	GN159_10580/ GPJ58_19035	3.6.1.63
	*phn*P	phosphonate metabolism protein PhnP	104206..104988	GPJ58_19020	3.1.4.55
	pdeH	cyclic-guanylate-specific phosphodiesterase	14132..14923	GPJ58_23400	-
	pdeR	cyclic di-GMP phosphodiesterase	5241..7235	GPJ58_23370	3.1.4.52

3.3. Model Quality of Pesticide-Degrading Proteins in *Serratia* sp. HSTU-ABk35

The pesticide-degrading protein models for *Serratia* sp. HSTU-ABk35 were evaluated using a variety of parameters, as shown in **Table 4**. A total of 29 model proteins were generated using the template-based method in "I-TASSER". When assessing the quality of the protein models; TM score, RMSD, Identity (Iden.), Coverage (cov.), orientation of secondary structures (α-helix, β–strand, η–coil & disordered), "ERRAT" score (quality score based on non-bonded interactions of different types of atom), "VERIFY 3D" (verification of 3D representation according to refined structures from PDB) and Ramachandran plot (core, allowed, generously allowed and disallowed %) analyses were taken into account. The average TM score for the 29 models was 0.92, while the median was 0.93. Additionally, the most common values (mode) were 0.96, which is an indication of the excellent quality of the models. The mean, median, and mode values for all the quality parameters were calculated subsequently to get a general idea of the results found. The mean and median of the quality score in ERRAT came out as 79.35 and 84.01, RMSD came out as 0.61 and 0.61, identity came out as 0.52 and 0.49, coverage came out as 0.89 and 0.91, α–helix came out as 32.76 and 32.0, β–strand came out as 20.07 and 20.0, η–coil came out as 45.90 and 46.5, disordered came out as 7.21 and 3.5, VERIFY (3D-ID score) % came out as 82.28 and 83.44 and Ramachandran plot (core, allow, gener, disallow) % came out as 81.06, 15.34, 2.16, 1.45 and 82.3, 15.17, 1.75, 1.3 which are optimal while 3D-1D verification in "VERIFY3D". Notably 18 proteins that are VERIFY (3D-ID score) above 80% are green and 11 proteins that are VERIFY (3D-ID score) below 80% are purple.

Table 4. Model quality of pesticide degrading protein *Serratia* sp. HSTU-ABk35.

List	Model protein	Best PDB hit	TM score, RMSD, Identity, coverage	α -helix, β –strand, η-coil, disordered	ERRAT (quality score)	VERIFY (3D-ID score) %	Ramachandran plot (core, allow, gener, disallow) %
1.	*AmpD*	1j2s	0.93, 0.49, 0.71, 0.94	24, 15, 60, 10	77.36	89.39	57.0, 35.8, 5.5, 1.8
2.	*glpA*	2rgo	0.91, 0.54, 0.67, 0.88	35, 18, 46, 5	87.80	80.87	68.5, 22.1, 6.5, 2.9
3.	*GlpB*	1lpf	0.87, 0.46, 0.65, 0.93	27, 19, 52, 0	70.53	87.68	55.2, 32.5, 7.5, 4.9
4.	*glpQ*	1ydy	0.94, 0.43, 0.31, 0.91	32, 15, 52, 8	79.42	89.69	86.1, 12.0, 1.3, 0.6
5.	*OpdE*	6kki	0.91, 0.48, 0.29, 0.91	80, 0, 19, 100	98.21	78.75	89.9, 7.7, 1.2, 1.2
6.	*pdeH*	4rnf	0.93, 1.32, 0.18, 0.96	32, 18, 49, 12	88.23	70.34	85.9, 12.0, 1.7, 0.4
7.	*pdeR*	5xgb	0.81, 0.64, 0.27, 0.81	40, 25, 34, 1	79.87	75.45	72.2, 19.9, 4.4, 3.5
8.	*pepA*	1gyt	0.99, 0.23, 0.91, 1.00	33, 20, 46, 1	96.16	98.01	81.9, 15.5, 1.2, 1.4
9.	*PepB*	6cxd	0.96, 0.30, 0.845, 0.97	34, 20, 44, 0	93.06	88.50	82.3, 15.0, 1.6, 1.1
10.	*pepD*	3mru	0.84, 0.70, 0.55, 0.83	26, 25, 47, 3	85.44	96.08	83.4, 15.4, 1.0, 0.2
11.	*PepE*	1fye	0.87, 0.61, 0.36, 0.91	28, 27, 43, 0	82.58	98.28	88.2, 7.9, 2.0, 2.0
12.	*phnF*	2wv0	0.86, 0.57, 0.44, 0.92	28, 33, 38, 4	97.41	75.52	79.2, 18.1, 2.3, 0.5
13.	*phnG*	4xb6	0.82, 0.65, 0.29, 0.86	43, 27, 29, 4	92.75	73.47	84.4, 13.3, 0.0, 2.3
14.	*PhnH*	2fsu	0.84, 0.75, 0.53, 0.86	24, 21, 54, 3	95.67	90.16	74.4, 21.3, 1.8, 2.4
15.	*PhnI*	4xb6	0.96, 0.89, 0.78, 0.97	37, 13, 49, 11	89.27	54.85	78.8, 17.3, 2.3, 1.6
16.	*PhnJ*	4xb6	0.96, 0.27, 0.88, 0.96	24, 19, 56, 5	92.08	81.82	78.9, 17.5, 0.4, 3.3
17.	*PhnK*	4fwi	0.95, 0.73, 0.30, 0.96	33, 20, 46, 5	93.30	93.51	82.1, 15.7, 1.3, 0.9
18.	*PhnL*	5gko	0.92, 0.82, 0.32, 0.94	34, 25, 40, 2	91.03	87.88	80.0, 15.6, 2.9, 1.5
19.	*paaC*	1OTK	0.94, 0.81, 0.58, 0.85	27, 24, 48, 4	92.11	94.38	93.6, 5.9, 0.0, 0.5

20.	*M-10*	6I5S	0.83, 0.62, 0.41, 0.73	31, 17, 50, 12	38.15	69.43	75.6, 19.2, 3.6, 1.5
21.	*M-9*	2ICS	0.72, 0.68, 0.75, 0.81	27, 24, 48, 4	81.14	95.45	90.7, 8.6, 0.3, 0.3
22.	*M-8*	4DO7	0.91, 0.59, 0.73, 0.89	37, 14, 48, 3	89.78	99.65	88.5, 10.3, 0.4, 0.8
23.	*M-7*	4EWT	0.95, 0.76, 0.31, 0.79	35, 23, 41, 0	75.13	83.68	89.5, 9.3, 0.9, 0.3
24.	*M-6*	2ODF	0.84, 0.64, 0.41, 0.81	30, 15, 53, 6	78.60	85.66	89.5, 9.6, 1.0, 0.0
25.	*M-5*	5XOY	0.99, 0.54, 0.81, 1.00	31, 22, 45, 3	52.81	66.49	82.4, 13.7, 3.0, 0.9
26.	*M-4*	2E11	0.96, 0.35, 0.84, 0.93	21, 33, 45, 1	77.82	83.20	89.2, 9.9, 0.9, 0.0
27.	*M-3*	2QYV	0.86, 0.78, 0.45, 0.83	34, 23, 42, 1	44.00	71.74	76.3, 18.1, 2.5, 3.1
28.	*M-2*	1M22	0.77, 0.69, 0.36, 0.96	35, 11, 53, 1	56.31	79.53	84.8, 12.7, 2.3, 0.3
29.	*M-1*	2FTY	0.96, 0.27, 0.34, 0.81	28, 16, 54, 0	25.27	46.80	82.3, 13.1, 2.8, 1.8

*[M-1= a*midohydrolase* family protein (locus_tag="GPJ58_05060), M-2= *AtzE* family *amidohydrolase* (locus_tag="GPJ58_08375) M-3= *allantoate amidohydrolase* (locus_tag="GPJ58_08420), M-4= *amidohydrolase* (locus_tag="GPJ58_08425), M-5= *amidohydrolase* (locus_tag="GPJ58_09790), M-6= *N-formylglutamate amidohydrolase* (locus_tag="GPJ58_11345), M-7= *amidohydrolase* (locus_tag="GPJ58_11730), M-8= *amidohydrolase* family protein (locus_tag="GPJ58_12900), M-9= *amidohydrolase/deacetylase* family *metallohydrolase* (locus_tag="GPJ58_14960), M-10= *amidohydrolase* family protein (locus_tag="GPJ58_17120)]

3.4. Virtual screening and box plot of complex

The virtual screening of the selected eighteen model proteins of *Serratia* sp. strain HSTU-ABK35, with ninety-nine different pesticides, shown binding score ranges from -9 Kcal/mol to -3 Kcal/mol (**Figure 3**). It is shown that most of the binding scores are occupied between the 1st and 3rd quartile in the box plot (**Figure 3)**, where the lower and upper quartile designates the 1st and 3rd quartile scores. Interestingly, three model proteins (PaaC, GlpA, PhnK) of *Serratia* sp. HSTU-ABk35, and two model proteins (AmpD, PepA) binding score were placed outlier data points. The virtual screening results also showed that the binding affinity of many pesticide ligands crossed over to -6.5~8.0 Kcal/mol for organophosphate degrading potential proteins (Amidohydrolase variants, PaaC, AmpD, GlpA, GlpB, GlpQ, and various Pep and Phn proteins) from *Serratia* sp. HSTU-ABk35 **(Figure 3).**

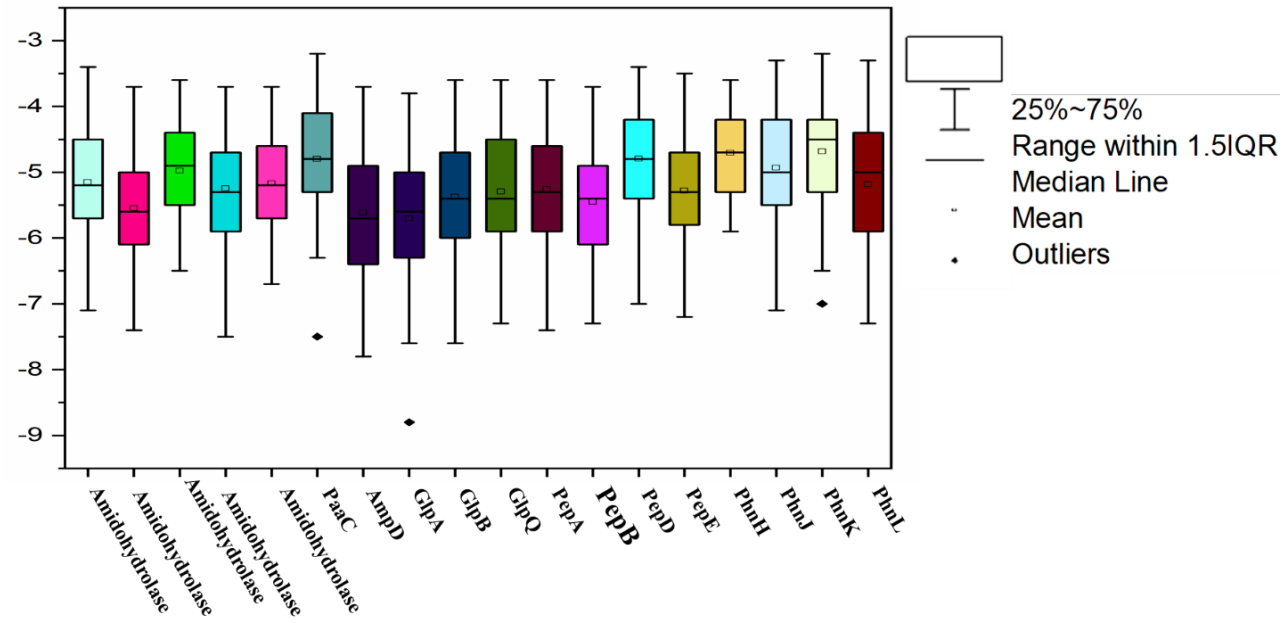

Figure 3. virtual screening analysis of ninety-nine pesticides with pesticide degrading model proteins of *Serratia* sp. Strain HSTU-Abk35.

3.5. Molecular docking of top four selected protein-pesticide complex

In this circumstance, all the ligand molecules are observed to follow Lipinski's rule of five (molecular weight not more than 500 Da; hydrogen bond donor not more than 5; hydrogen bond acceptors not more than 10; log p-value not greater than 5). The 2D and 3D interactions of the four selected ligands with four proteins after docking show the active sites of the receptor were visualized by using biovia discovery studio and chimera. The 2D and 3D catalytic interactions of the selected two proteins catalytically important residues according to docking analyses are placed within 1.5–5.5Å that might play a role in the degradation of organophosphate pesticides. The GlpQ protein with a Chlorpyrifos docked complex demonstrated the interaction with multiple residues (**Figure 4A**). In particular, conventional H-bonds were made by the Arg33 and Arg313 to the benzene ring attached, S-atom. Besides, Asp75 formed π anion, Leu 231 formed an alkyl, Phe310 and Trp237 formed π-sigma, Phe306 and His32 formed π-alkyl Halogen interacted with chlorpyrifos' Cl-atom and benzene ring. Interestingly, this dock was formed by the catalytic tired His32-Arg33-Asp75.

PaaC interacts with Cayanophenophos via multiple amino acid residues (**Figure 4B**). In fact, the O-atom in the phosphodister bond of Cayanophenophos is attacked by Asp47 via attractive charge interaction with the phosphate atom. Notably, the His137 and His137 residues provided combined, π-sulfur and carbon hydrogen bond interactions to the Cypermethrin compound, respectively. Attractively, this interacted to form a catalytic tire, His137-Arg139-Asp47.

Likewise, the GlpA with Cypermethrin docked complex showed multiple residue interactions (**Figure 4C**). The conventional hydrogen bond interaction was observed for Arg316 and Arg332 with the side chain of the benzene ring attached, the O-atom, and the N-H atom of the phosphodiester of Azinophos ethyl compound, while Lys355, Leu356, and Met356 formed alkyl and π-alkyl bonds with the Cl-atom of Azinophos ethyl, and Tyr61 formed.

The AmpD protein and Phoxim insecticide docked complex ligand interactions were observed by the different residues (**Figure 4D**). In particular, Glu127 with Asp170 provided an attractive charge interaction with the phosphate atom. The interaction distance was 4.77 and 4.87. In addition, conventional hydrogen bond and pi sigma interactions were observed with the Ala168 and Arg173 residues. The interaction distances among the residues of the catalytic site were recorded within <3.9 Å.

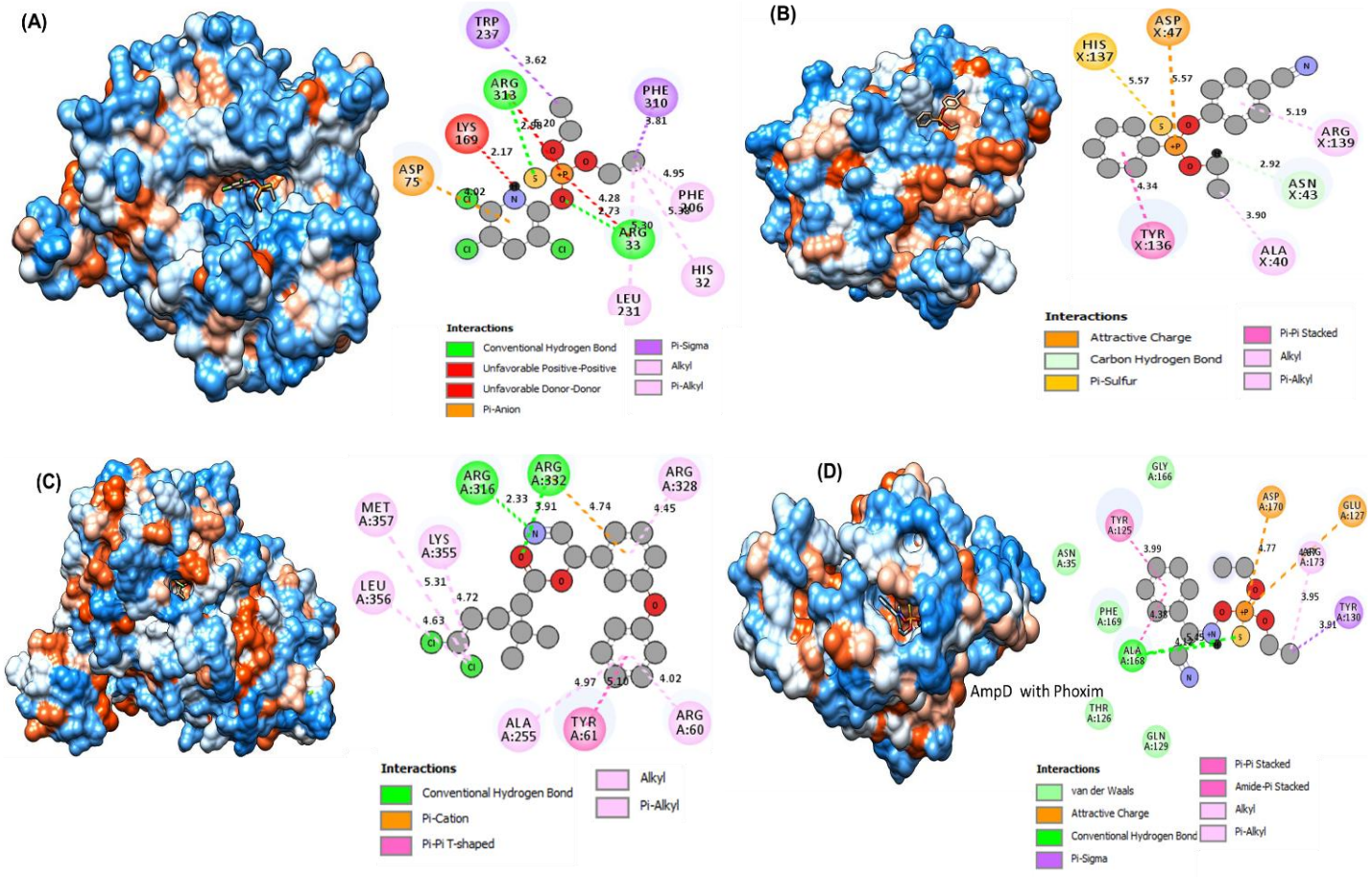

Figure 4. (A) Molecular docking and chemicals interactions of organophosphorus degrading model protein GlpQ of *Serratia* sp. Strain HSTU-Abk35 with chlorpyrifos pesticides. **(B)** Molecular docking and chemicals interactions of organophosphorus degrading model protein PaaC of *Serratia* sp. Strain HSTU-Abk35 with Cayanophenophos pesticides. **(C)** Molecular docking and chemicals interactions of organophosphorus degrading model protein GlpA of *Serratia* sp. Strain HSTU-Abk35 with Cypermethrin pesticides. **(D)** Molecular docking and chemicals interactions of organophosphorus degrading model protein AmpD of *Serratia* sp. strain HSTU-Abk35 with phoxim pesticides.

4. DISCUSSION

The comprehensive genomic and functional characterization of *Serratia* sp. HSTU-ABk35 reveals this strain as an ecologically versatile endophyte capable of simultaneously promoting plant health and degrading multiple classes of pesticides. The integration of whole-genome sequencing, phylogenomic analyses, gene repertoire profiling, structural modeling, and molecular docking establishes a robust framework for understanding its dual ecological and biotechnological significance. Such multi-layer genome-to-function approaches have been emphasized in recent studies exploring plant-associated bacteria with environmental or agricultural relevance [4, 2].

Genome-based phylogenetic analyses clearly placed *Serratia* sp. HSTU-ABk35 within the *Serratia marcescens* species complex, supported by high ANI and dDDH values consistent with species-level boundaries defined by Meier-Kolthoff et al. [27]. The clustering of housekeeping genes such as *recA* and *rpoB* with reference *S. marcescens* strains agrees with previous findings demonstrating the utility of these loci for fine-scale taxonomic discrimination within *Serratia* [11]. The subtle divergence observed in the *gyrB*-based clustering suggests microevolutionary adaptation, a pattern previously documented in *Serratia* strains exposed to environmental stressors or agrochemicals. Such genomic plasticity is often associated with niche adaptation among endophytes colonizing plant tissues [29].

Pan-genome comparison and locally collinear block analysis revealed several strain-specific genomic regions in *Serratia* sp. strain HSTU-ABk35, indicating acquisition of novel operons potentially through horizontal gene transfer. This aligns with reports of diverse *Serratia* lineages evolving specialized genetic modules for metabolic versatility in soil and plant-associated environments [30]. The presence of unique genomic islands containing xenobiotic-degradation and colonization-related genes parallels the genomic signatures observed in *Serratia plymuthica*, *S. nematodiphila*, and other environmental strains enriched for ecological adaptability [30]. Similar patterns of metabolic specialization have been described in endophytes and gut-associated bacteria such as *Klebsiella variicola*, where strains display niche-driven acquisition of lignocellulolytic and catabolic functions [17].

The plant-beneficial genetic repertoire of *Serratia* sp. HSTU-ABk35 includes genes associated with nitrogen metabolism, siderophore biosynthesis, ACC deaminase, phytohormone pathways, and stress response systems—traits widely reported to contribute to plant growth promotion and enhanced stress tolerance [2, 4, 31]. These functions resemble those of well-characterized endophytic *Serratia* strains that enhance crop growth, nutrient uptake, and systemic resistance [12, 32]. Genes associated with induced systemic resistance reflect mechanisms previously described for beneficial plant–microbe interactions mediated by microbial metabolites and volatiles [33]. The presence of multiple oxidative, osmotic, and heavy-metal stress tolerance operons further underscores the strain's ecological resilience, consistent with bacterial adaptation strategies reported under agricultural stress conditions [34].

One of the most notable characteristics of *Serratia* sp. strain HSTU-ABk35 is its large and diverse array of xenobiotic-degrading genes, including carboxylesterases, α/β-hydrolases, amidohydrolases, phosphonate-metabolizing operons, and enzymes associated with aromatic compound breakdown. These gene families are well known for their roles in the degradation of organophosphate, organochlorine, and pyrethroid pesticides [35-38].

The presence of *ampD*, *glpA*, *glpB*, *glpQ*, and *pep* operons resembles enzymatic systems reported to mineralize chlorpyrifos, diazinon, methyl parathion, cypermethrin, and other toxic agrochemicals [3, 4]. The degradative capacities inferred here are also consistent with recent studies discovering novel pesticide-hydrolyzing esterases from rumen metagenomes [23] and biodegradation traits present in lactic acid bacteria and related taxa [36]. The genetic convergence between HSTU-ABk35 and other pesticide-mineralizing endophytes demonstrates clear evolutionary pathways for adapting to agrochemical-intensive environments [1].

This study leveraged a comprehensive computational approach to identify and characterize putative pesticide-degrading enzymes from *Serratia* sp. strain HSTU-ABk35. The findings offer significant insights into the structural characteristics and interaction mechanisms of these bacterial proteins with various agricultural pesticides. The initial phase involved the prediction of three-dimensional enzyme structures through homology modeling, followed by rigorous validation. The consistently high quality of the models-confirmed by excellent ERRAT and VERIFY-3D scores and favorable Ramachandran plot analyses-established a robust foundation for subsequent computational investigations [25, 3, 37]. This rigorous validation ensures the structural reliability necessary for accurate predictions of enzyme-substrate interactions. Virtual screening revealed a broad capacity among the identified enzymes to bind pesticide compounds. Notably, many proteins with organophosphate-degrading potential across all three bacterial strains, including amidohydrolase variants, PaaC, AmpD, Glp, and Pep/Phn proteins, exhibited strong binding affinities, frequently falling within the -6.5 to -8.0 Kcal/mol range. The identification of outlier interactions further points to exceptionally strong and specific binding events for certain protein-pesticide pairs [3, 4, 32, 37, 38]. This widespread and potent binding capability highlights these bacterial enzymes as promising candidates for pesticide recognition and detoxification. Detailed molecular docking provided atomic-level insights into these crucial interactions. Analysis elucidated specific amino acid residues involved in stabilizing the protein-pesticide complexes through various bond types, such as conventional hydrogen bonds, hydrophobic contacts, and pi-interactions. A particularly noteworthy finding was the identification of potential catalytic triads within the binding pockets. These specific arrangements of amino acids are characteristic of enzymatic active sites and play a critical role in facilitating chemical catalysis, strongly suggesting an active degradative function for these proteins.

In conclusion, this genomic and computational investigation provides a comprehensive characterization of pesticide-degrading protein models from the endophytic bacteria. The robust models, strong pesticide binding affinities, and the identification of potential catalytic sites collectively underscore the significant potential of these enzymes as novel biocatalysts for environmental bioremediation.

5. CONCLUSION

The genomic and functional characterization of *Serratia* sp. HSTU-ABk35 underscores its status as a novel endophytic strain within the *Serratia marcescens* complex, exhibiting measurable evolutionary divergence from known reference strains. The strain harbors a comprehensive repertoire of plant growth-promoting genes, including those for phytohormone production, nutrient mobilization, stress tolerance, and induction of systemic resistance, suggesting its robust potential to enhance crop health under variable environmental conditions. In parallel, the presence of a diverse suite of xenobiotic-

degrading genes, combined with in silico validation of enzyme–pesticide interactions, indicates its capacity to biotransform multiple classes of pesticides. These dual functionalities position *Serratia* sp. HSTU-ABk35 as a promising candidate for microbial inoculants aimed at sustainable agriculture, offering both enhancement of plant productivity and mitigation of agrochemical residues. Future experimental studies, including greenhouse and field trials, are warranted to validate its agricultural performance and bioremediation efficacy.

ACKNOWLEDGEMENTS

The authors gratefully acknowledge IRT of Hajee Mohammad Danesh Science and Technology University (HSTU), for financial support. We also thank all contributors for their valuable roles in the preparation of this manuscript. This study addresses about 10% AI-assisted text following the journal policy.

FUNDING SOURCES

This research was supported by the grants from the Institute of Research and Training (IRT)-Hajee Mohammad Danesh Science and Technology University (HSTU) in fiscal year 2021-2022 at Dinajpur, Bangladesh.

CONFLICTS OF INTEREST

The authors declare no conflicts of interest.

ETHICS STATEMENT

This study did not involve any experiments on human participants or animals; therefore, formal written informed consent was not required by the Institutional Review Board. All figures in this study were created; therefore, no permission for reuse is required for any figure presented herein.

DATA AVAILABILITY STATEMENT

The assembled and annotated genome sequence of *Serratia* sp. strain HSTU-ABk35, isolated from rice plant roots, was deposited in the NCBI database under the accession number WSPF00000000, with BioSample SAMN13520210 and BioProject PRJNA594520.

REFERENCES

1. Haque MA, Simo, Prodhan MY, Ghosh S, Hossain MS, Rahman A, Haque MA. Enhanced rice plant (BRRI-28) growth at lower doses of urea caused by diazinon mineralizing endophytic bacterial consortia and explorations of relevant regulatory genes in a *Klebsiella* sp. strain HSTU-F2D4R. *Arch Microbiol*. 2023;*205*(6):231. https://doi.org/10.1007/s00203-023-03564-2
2. Prodhan MY, Rahman MB, Rahman A, Akbor MA, Ghosh S, Nahar MNEN, ... Haque MA. Characterization of growth-promoting activities of Consortia of Chlorpyrifos mineralizing endophytic bacteria naturally harboring in rice plants—a potential bio-stimulant to develop a safe and sustainable agriculture. *Microorganisms*. 2023;*11*(7): 1821. https://doi.org/10.3390/microorganisms11071821
3. Das SR, Haque MA, Akbor MA, Abdullah-Al-Mamun M, Debnath GC, Hossain MS, ... Cho KM. Organophosphorus insecticides mineralizing endophytic and rhizospheric soil bacterial consortium influence eggplant growth-promotion. *Arch Microbiol*. 2022; *204*(3):199. https://doi.org/10.1007/s00203-022-02809-w
4. Haque MA, Hossain MS, Ahmad I, Akbor MA, Rahman A, Manir MS, Cho KM. Unveiling chlorpyrifos mineralizing and tomato plant-growth activities of *Enterobacter* sp. strain HSTU-ASh6 using biochemical tests, field experiments, genomics, and in silico analyses. *Front Microbiol*. 2022. *13*, 1060554. https://doi.org/10.3389/fmicb.2022. 1060554
5. Cho DY, Jang MY, Lee HY, Jeong JB, Kim DH, Bang DY,Cho KM. Rhizospheric bacterial distribution influencing the accumulation of isoflavones, phenolics, flavonoids, and antioxidant activity in soybean roots within hydroponic system. *Plants*. 2025;*14*(14): 2238. https://doi.org/10.3390/plants14142238
6. Chaudhary P, Agri U, Chaudhary A, Kumar A, Kumar G. Endophytes and their potential in biotic stress management and crop production. *Front Microbiol*. 2022;13: 933017. doi: 10.3389/fmicb.2022.933017
7. Cho DY, Haque MA, Lee HY, Jang MY, Jeong JB, Lee GY, Cho KM. Amending metagenomic bacterial community in soybean-cultivated soils to enhance phytoestrogen in soybean roots by communicating with mixture of culturable rhizospheric racteria. https://dx.doi.org/10.2139/ssrn.5174384
8. Christiansen S, Bendevis MA. 2018. Plant Biology Europe 2018 Conference : Abstract Book. In *Research Portal Denmark* (p. 479). Technical University of Denmark. https://local.forskningsportal.dk/local/dki-cgi/ws/cris-link?src=ku&id=ku-25f1207b-a965-4ecc
9. Sallam NM, AbdElfatah HAS, Khalil Bagy HM, Elfarash A, Abo-Elyousr KA, Sikora E J, Sallam A. Exploring the mechanisms of endophytic bacteria for suppressing early blight disease in tomato (*Solanum lycopersicum* L.). *Front. Microbiol.* 2023; 14: 1184343. https://doi.org/10.3389/fmicb.2023.1184343
10. Hugouvieux-Cotte-Pattat N, Jacot-des-Combes C, Briolay J. Genomic characterization of a pectinolytic isolate of Serratia oryzae isolated from lake water. *J genomics*. 2019; *7*, 64. https://doi.org/10.7150/jgen.38365
11. Khan AR, Park GS, Asaf S, Hong SJ, Jung BK, Shin JH. Complete genome analysis of *Serratia marcescens* RSC-14: A plant growth-promoting bacterium that alleviates cadmium stress in host plants. *PloS one*. 2017;*12*(2), e0171534. https://doi.org/10.1371/journal.pone.0171534
12. Lee J, Kim S, Jung H, Koo BK, Han JA, Lee HS. Exploiting bacterial genera as biocontrol agents: Mechanisms, interactions and applications in sustainable agriculture. *Journal of Plant Biology*. 2023; *66*(6), 485-498. https://doi.org/10.1007/s12374-023-09404-6
13. Chlebek D, Grebtsova V, Piński A, Żur-Pińska J, Hupert-Kocurek K. Genetic determinants of antagonistic interactions and the response of new endophytic strain *Serratia quinivorans* KP32 to fungal phytopathogens. *Int J Mol Sci*. 2022; *23*(24), 15561. https://doi.org/10.3390/ijms232415561
14. Marques-Pereira C, Proença DN, Morais PV. Genome sequences of *Serratia* strains revealed common genes in both serratomolides gene clusters. *Biology*. 2020; *9*(12): 482. https://doi.org/10. 3390/biology9120482
15. Matteoli FP, Passarelli-Araujo H, Reis RJA, Da Rocha LO, De Souza EM, Aravind L, Venancio TM. Genome sequencing and assessment of plant growth-promoting properties of a Serratia marcescens strain isolated from vermicompost. *BMC genomics*. 2018. *19*(1), 750. https://doi.org/10.1186/s12864-018-5130-y
16. Alatassi G, Baysal Ö, Silme RS, Örnek GP, Örnek H, Can A. Pesticide degradation capacity of a novel strain belonging to *Serratia sarumanii* with its genomic profile. *Biodegradation*. 2018; *36*(3): 49. https://doi.org/10.1007/s10532-025-10144-2
17. Abdullah-Al-Mamun M, Hossain MS, Debnath GC, Sultana S, Rahman A, Hasan Z. Haque MA. Unveiling lignocellulolytic trait of a goat omasum inhabitant *Klebsiella variicola* strain HSTU-AAM51 in light of biochemical and genome analyses. *Braz J Microbiol*. 2022; *53*(1): 99-130. https://doi.org/10.1007/s42770-021-00660-7
18. Zeng B, Zhang F, Liu YT, Wu SF, Bass C, Gao CF. Symbiotic bacteria confer insecticide resistance by metabolizing buprofezin in the brown planthopper, Nilaparvata lugens (Stål). *PLoS Pathogens*. 2023; *19*(12):e1011828.). https://doi.org/10.1371/journal.ppat.1011828

19. Renoz F, Foray V, Ambroise J, Baa-Puyoulet P, Bearzatto B, Mendez GL, Hance T. At the gate of mutualism: identification of genomic traits predisposing to insect-bacterial symbiosis in pathogenic strains of the aphid symbiont *Serratia symbiotica*. Front. Cell. Infect. Microbiol. 2021; 11: 660007. https://doi.org/10.3389/fcimb.2021.660007

20. Vaughan AL, Altermann E, Glare TR, Hurst MR. Genome sequence of the entomopathogenic *Serratia entomophila* isolate 626 and characterisation of the species specific itaconate degradation pathway. *BMC genomics*. 2022; *23*(1): 728. https://doi.org/10.1186/s12864-022-08938-2

21. Sharker B, Islam MA, Hossain MAA, Ahmad I, Al Mamun A, Ghosh S, Haque MA. Characterization of lignin and hemicellulose degrading bacteria isolated from cow rumen and forest soil: Unveiling a novel enzymatic model for rice straw deconstruction. *Sci. Total Environ*. 2023. *904*, 166704. https://doi.org/10.1016/j.scitotenv.2023.166704

22. Haque MA, Lee JH, Cho KM. Endophytic bacterial diversity in Korean kimchi made of Chinese cabbage leaves and their antimicrobial activity against pathogens. *Food Control*. 2015; *56:* 24-33. https://doi.org/10.1016/j.foodcont.2015.03.006

23. Lee HY, Cho DY, Ahmad I, Patel HM, Kim MJ, Jung JG, Cho KM. Mining of a novel esterase (*est*3S) gene from a cow rumen metagenomic library with organosphosphorus insecticides degrading capability: Catalytic insights by site directed mutations, docking, and molecular dynamic simulations. *Int J Biol Macromol*. 2021;*190*: 441-455. https://doi.org/10.1016/j.ijbiomac.2021.08.224

24. Lee JH, Lee HY, Cho DY, Kim MJ, Jung JG, Jeong EH., Cho KM. Biodegradable properties of organophosphorus insecticides by the potential probiotic *Lactobacillus plantarum* WCP931 with a degrading gene (opd C). *Appl Biol Chem*. 2021. *64*(1), 62. https://doi.org/10.1186/s13765-021-00632-3

25. Ramzan K, Sabri S, Alshaya DS, Ramzan S, Khan MS, Abbas F., Murtaza M. Homology modelling and structural docking analysis on a human BDNF gene by using Computational algorithms. 2024. https://doi.org/ 10.21203/rs.3.rs-5294979/v1

26. Haque MA, Barman DN, Rahman A, Hossain MS, Ghosh S, Nahar MA, Nahar MN, Saha JK, Cho KM, Yun HD. Molecular cloning, in silico analysis, and characterization of a novel cellulose microfibril swelling gene isolated from *Bacillus* sp. strain AY8. Microorganisms. 2023;24;11(12):2857. doi: 10.3390/microorganisms11122857

27. Barua H, Hasan MR, Mardiya RT, Shishir TA, Hossain H, Azam FMS, Akhand MRN, Mashrur MN. Developing a novel multi-epitope subunit vaccine to combat monkeypox virus through an immunoinformatics approach. Vacunas. 2025,500490. https://doi.org/10.1016/j.vacun.2025.500490

28. Meier-Kolthoff JP, Auch AF, Klenk HP, Göker M. Genome sequence-based species delimitation with confidence intervals and improved distance functions. *BMC bioinformatics*. 2013. *14*(1), 60. https://doi.org/10.1186/1471-2105-14-60

29. Hardoim PR, Van Overbeek LS, Berg G, Pirttilä AM, Compant S, Campisano A., Sessitsch A. The hidden world within plants: ecological and evolutionary considerations for defining functioning of microbial endophytes. *Microbiol Mol Biol Rev*. 2015;*79*(3):293-320. https://doi.org/10.1128/mmbr.00050-14

30. Yu Y, Gui Y, Li Z, Jiang C, Guo J, Niu D. Induced systemic resistance for improving plant immunity by beneficial microbes. *Plants.* 2022;*11*(3):386. https://doi.org/10.3390/plants11030386

31. Basharat Z, Tanveer F, Yasmin A, Shinwari ZK, He T, Tong Y. Genome of *Serratia nematodiphila* MB307 offers unique insights into its diverse traits. *Genome*. 2018; *61*(7), 469-476.doi: 10.1139/gen-2017-0250

32. Sharma N, Mahawar L, Mishra A, Albrectsen BR. Microbial contributions to plant growth and stress tolerance: mechanisms for sustainable plant production. *Plant Stress*. 2025. 100966. https://doi.org/10.1016/j.stress. 2025.100966

33. Gyaneshwar P, Naresh Kumar G, Parekh LJ, Poole PS. Role of soil microorganisms in improving P nutrition of plants. *Plant and soil*. 2002; *245*(1): 83-93. https://doi.org/10.1023/A:1020663916259

34. Meena KK, Sorty AM, Bitla UM, Choudhary K, Gupta P, Pareek A., Minhas PS. Abiotic stress responses and microbe-mediated mitigation in plants: the omics strategies. *Frontiers in plant science*. 2017. *8*, 172. doi: 10.3389/fpls.2017.00172

35. Haque MA, Hossain MS, Ahmad I, Akbor MA, Rahman A, Manir MS., Cho KM. Unveiling chlorpyrifos mineralizing and tomato plant-growth activities of *Enterobacter* sp. strain HSTU-ASh6 using biochemical tests, field experiments, genomics, and *In silico* analyses. *Front Microbiol*. 2022.*13*, 1060554. https://doi.org/10.3389/fmicb.2022. 1060554

36. Haque AM, Hwang CE, Kim SC, Cho DY, Lee HY, Cho KM, Lee JH. Biodegradation of organophosphorus insecticides by two organophosphorus hydrolase genes (opdA and opdE) from isolated *Leuconostoc mesenteroides* WCP307 of kimchi origin. *Process Biochem*. 2020. *94*, 340-348. https://doi.org/10.1016/j.procbio.2020.04.026

37. Haque MA, Hong SY, Hwang CE, Kim SC, Cho KM. Cloning of an organophosphorus hydrolase (opdD) gene of Lactobacillus sakei WCP904 isolated from chlorpyrifos-impregnated kimchi and hydrolysis activities of its gene product for organophosphorus pesticides. *Applied Biological Chemistry*. 2018. *61*(6), 643-651. doi:10.1007/s 13765-018-0397-x

38. Barman DN, Haque MA, Islam SMA, Yun HD, Kim MK. Cloning and expression of *oph*B gene encoding organophosphorus hydrolase from endophytic Pseudomonas sp. BF1-3 degrades organophosphorus pesticide chlorpyrifos. *Ecotoxicol Environ Saf*. 2014. *108*, 135-141. https://doi.org/10.1016/j.ecoenv.2014.06.023